Chlorine isotope fractionation during serpentinization and hydrothermal mineralization: A density functional theory study

Xi Liu [a], Hai-Zhen Wei [a,e] *, A. E. Williams-Jones [b], Jing Ma [c], Jian-Jun Lu [a], Shao-Yong Jiang [d], Yin-Chuan Li [a], Ge Dong [a]

[a] *State Key Laboratory for Mineral Deposits Research, Department of Earth Sciences and Engineering, Nanjing University, Nanjing 210023, PR China*

[b] *Department of Earth and Planetary Sciences, McGill University, Montreal H3A 0E8, Canada*

[c] *Key Laboratory of Mesoscopic Chemistry of MOE, School of Chemistry & Chemical Engineering, Nanjing University, Nanjing, 210023, PR China*

[d] *State Key Laboratory of Geological Processes and Mineral Resources, Faculty of Earth Resources, China University of Geosciences, Wuhan 430074, PR China*

[e] *CAS Center for Excellence in Comparative Planetology, China, Anhui 230026, PR China*

* Author to whom correspondence should be addressed:
Prof. Hai-Zhen Wei
School of Earth Sciences and Engineering, Nanjing University
163 Xianlin Avenue, Nanjing, Jiangsu, 210023 PR China
Phone: +86 (25) 89681617; Fax: +86 (25) 89682393
Email address: haizhenwei@nju.edu.cn

Liu, X., Wei, H.-Z., Williams-Jones, A., Ma, J., Lu, J.-J., Jiang, S.-Y., Li, Y.-C., and Dong, G., 2021,
Chlorine isotope fractionation during serpentinization and hydrothermal mineralization: A density functional theory study:
Chemical Geology, v. 581, p. 120406.

ABSTRACT

Because of the large-scale recycling of volatile chlorine from the interior to the surface of the Earth, it is possible to use the isotopic composition of this element ($\delta^{37}Cl$) in serpentinite to study mantle-crust interactions in subduction zones. It is also possible to use chlorine isotopes to track the evolution of fluids (through fluid inclusions/minerals) in hydrothermal ore-forming systems. Here, we report the results of a study of equilibrium chlorine isotope fractionation during serpentinization and hydrothermal mineralization based on density functional theory (DFT) and *ab initio* molecular dynamics simulations (AIMD). The chlorine isotope fractionation between lizardite and brine under variable thermodynamic conditions is described by the relationship $1000\ln\alpha_{\text{lizardite-fluid}} = 0.4170 \times (1000/T)^2 - 0.0281\times (1000/T) + 0.0582$, which yielded $\Delta^{37}Cl_{\text{lizardite-fluid}}$ values of +0.49 to +4.46‰, +0.37 to +0.59‰ and +0.49 to +3.57‰ for conditions at the seafloor, in the mantle wedge and in subduction zones. As a proxy for the diversity of metal-chloride complexes in hydrothermal fluids, the stable configurations of ferrous chloride complexes were acquired from long trajectories of AIMD simulation. Using this information, the chlorine isotope fractionation between minerals (i.e., apatite-group minerals, muscovite, phlogopite, tremolite, lizardite, marialite and metal halides) and ore-forming fluid was estimated. The relatively large chlorine isotope fractionation ($\Delta^{37}Cl_{\text{minerals-hydrothermal fluid}}$ values from -1.99 to +2.18‰) might partly explain the large variation of $\delta^{37}Cl$ in individual fluid inclusions observed in hydrothermal ore deposits. Because of the limited chlorine isotope fractionation between apatite and hydrothermal fluid (i.e., $\Delta^{37}Cl_{\text{apatite-ore-forming fluid}}$ of 0.06‰ - 0.69‰), apatite-group minerals might be an alternative to fluid inclusions for constraining the origin and evolution of hydrothermal fluids using $\delta^{37}Cl$ values. The theoretical constraints provided in this paper will facilitate the use of chlorine isotopes in tracking the sources of chloride in subduction zones and the origin of mineralizing fluids in ore deposits.

Keywords: Equilibrium chlorine isotope fractionation; chlorine-bearing minerals; serpentinization; hydrothermal mineralization

Liu, X., Wei, H.-Z., Williams-Jones, A., Ma, J., Lu, J.-J., Jiang, S.-Y., Li, Y.-C., and Dong, G., 2021,
Chlorine isotope fractionation during serpentinization and hydrothermal mineralization: A density functional theory study:
Chemical Geology, v. 581, p. 120406.

INTRODUCTION

Chlorine is a volatile and strongly hydrophilic element. It has two stable isotopes, ^{35}Cl with 18 neutrons and ^{37}Cl with 20 neutrons (Aston, 1919). The natural relative abundances of the two stable chlorine isotopes, ^{35}Cl and ^{37}Cl, are 75.76% and 24.24%, respectively (Berglund and Wieser, 2011). During the past two decades, studies of the chlorine cycle on Earth have advanced considerably (e.g., Eastoe et al., 2001; Eastoe, 2016; Sharp and Barnes, 2004; Barnes and Sharp, 2006; Barnes et al., 2006, 2008, 2009; Bonifacie et al., 2007, 2008; Shouakar-Stash et al., 2007; Selverstone and Sharp, 2011; Sharp et al., 2007, 2010b, 2013ab; Eggenkamp, 2014; Eggenkamp et al., 2016, 2019a, 2019b, 2020; Li et al., 2015; Pinti et al., 2020; Bénard et al., 2020; Agrinier et al., 2019, 2021), leading to an understanding of the processes controlling chlorine isotope variation (e.g., Sharp et al., 2010a). In addition, great progress has been made in theoretical simulations of equilibrium stable isotope fractionation among a variety of phases for a large number of elements, including chlorine (Balan et al., 2018, 2019; Huang et al., 2013, 2014, 2019; Schauble, 2007, 2011; Schauble and Young, 2021).

Serpentinized oceanic mantle lithosphere is an important carrier of water and fluid-mobile elements, including halogens, into subduction zones (Pagé and Hattori, 2019). The uptake of Cl by serpentinites is highly variable and is influenced by several factors, including water/rock ratio, salinity, the nature of the primary minerals (i.e., olivine and/or pyroxene) and temperature (Pagé and Hattori, 2019). In situ analyses of serpentine grains from modern seafloor and subducted abyssal serpentinites show that the concentrations of structurally bound Cl cover a large range (80 to 6000 ppm) and average ~1500 ppm (Orberger et al., 1999; Anselmi et al., 2000; Scambelluri et al., 2004; Debret et al., 2014; Pagé and Hattori, 2019), depending on the temperature of serpentinization. Therefore, serpentinites are thought to contribute significantly to the Cl concentration and the Cl isotopic composition of arc magmas (Barnes et al., 2008, 2009; Barnes and Straub, 2010; Bonifacie et al., 2008), which have been shown to be enriched in Cl relative to MORB (Kent et al., 2002; Perfit et al., 1980; Straub and Layne, 2003; Sun et al., 2007; Wallace, 2005; John et al., 2011). The stable

Liu, X., Wei, H.-Z., Williams-Jones, A., Ma, J., Lu, J.-J., Jiang, S.-Y., Li, Y.-C., and Dong, G., 2021,
Chlorine isotope fractionation during serpentinization and hydrothermal mineralization: A density functional theory study:
Chemical Geology, v. 581, p. 120406.

84 isotopes of chlorine have been used to identify the sources of serpentinizing fluids and discern
85 chemical and tectonic processes involved in serpentinization (Barnes and Sharp, 2006; Barnes et al.,
86 2006, 2008, 2009; Barnes and Straub, 2010; Rizzo et al., 2013; Barnes et al., 2013; Chiaradia et al.,
87 2014). For example, Manzini et al. (2017) showed that $\delta^{37}Cl$ in melt inclusions is a valuable tool for
88 constraining the origin of the Cl added to the mantle wedge, and that it can be used to refine current
89 models of Cl redistribution into the crust-mantle system related to subduction zone processes. A
90 combination of oxygen, boron and chlorine isotope analyses have shown that Cl is added to the
91 mantle wedge from several sources, rather than from a single reservoir (Bouvier et al., 2019). The
92 $\delta^{37}Cl$ values of serpentinites are affected by factors, such as the chlorine isotopic composition of the
93 serpentinizing fluid, the temperature of interaction, and the water/rock ratio (Barnes et al., 2013). In
94 order to properly understand chlorine cycling and the complex exchanges among the various
95 terrestrial reservoirs, it is therefore essential to be able to quantify the equilibrium chlorine isotope
96 fractionation during serpentinization.

97 In hydrothermal ore-forming processes, the transport of metals is governed by their complexation
98 with inorganic and organic ligands such as Cl^-, SO_4^{2-}, S^{2-}, NH_3^-, CO_3^{2-}, acetate, and propionate
99 (Wood and Samson, 1998). Chloride is the dominant ligand in most hydrothermal fluids (Fein et al.,
100 1992; Bodnar et al., 2014; Scholten et al., 2019), and plays an essential role in the mobilization of
101 metals from magmas by fluids (Eggenkamp et al., 1995; Marakushev et al., 1997; Ryabov et al.,
102 2018). Indeed, the concentration of chloride in hydrothermal fluids greatly affects the efficiency of
103 extraction of metals from magmas and their transportation to the sites of ore deposition (Williams-
104 Jones and Migdisov, 2014; Gammons and Williams-Jones, 1995; Xiao et al., 1998). Therefore,
105 knowledge of its behavior is indispensable in understanding the origin of magmatic-hydrothermal
106 ore deposits (e.g., Candela and Holland, 1984; Hedenquist and Lowenstern, 1994; Williams-Jones
107 and Heinrich, 2005).

Liu, X., Wei, H.-Z., Williams-Jones, A., Ma, J., Lu, J.-J., Jiang, S.-Y., Li, Y.-C., and Dong, G., 2021,
Chlorine isotope fractionation during serpentinization and hydrothermal mineralization: A density functional theory study:
Chemical Geology, v. 581, p. 120406.

A potentially important means of gaining greater insight into the behavior of chlorine in hydrothermal fluids, including those of magmatic origin, is through studies of their chlorine isotope composition. Indeed, a number of studies have used the chlorine isotope composition of fluid inclusions to try and constrain the evolution of fluids in hydrothermal ore-forming systems (e.g., Eastoe et al., 1989; Eastoe and Guilbert, 1992; Banks et al., 2000; Bonifacie et al., 2005; Chiaradia et al., 2006; Gleeson and Smith, 2009; Nahnybida et al., 2009; Richard et al., 2011; Hanley et al., 2011; Selley et al., 2018). However, the factors controlling the behavior of chlorine isotopes in these systems remains poorly understood, in large part, because of a lack of information on their fractionation.

In this work, the equilibrium chlorine isotope fractionation during serpentinization and hydrothermal mineralization has been evaluated using theoretical first-principles calculations. The objectives of the present study are: i) to quantify temperature-dependent equilibrium chlorine isotope fractionation between lizardite and brine during serpentinization; ii) to determine the stable configurations of ferrous chloride complexes, and then evaluate chlorine isotope fractionation between chlorine-bearing accessory minerals and these complexes in hydrothermal fluids during ore-formation; and iii) to assess the potential of using $\delta^{37}Cl$ in minerals to trace the source of ore-forming fluids and evaluate the chlorine cycle during subduction.

2. COMPUTATIONAL METHODS

2.1 Equilibrium isotopic fractionation factors

The theory of Bigeleisen and Mayer (1947), Kieffer (1982), and Urey (1947), stipulates that the dependence of the vibrational frequencies on isotopic mass on molecular bonds leads to isotope fractionation. For a chlorine isotope exchange reaction, if there is only one chlorine atom in substance X and n chlorine atoms in substance Y, this exchange reaction is:

Liu, X., Wei, H.-Z., Williams-Jones, A., Ma, J., Lu, J.-J., Jiang, S.-Y., Li, Y.-C., and Dong, G., 2021,
Chlorine isotope fractionation during serpentinization and hydrothermal mineralization: A density functional theory study:
Chemical Geology, v. 581, p. 120406.

132 $$nX + Y^* \leftrightarrow nX^* + Y \qquad \text{(Eq. 1)}$$

133 where X and Y identify the substances containing the lighter isotope (^{35}Cl), X* and Y* identify the
134 substances containing the heavier isotope (^{37}Cl) and n is the number of chlorine atoms (^{37}Cl)
135 substituted in Y*. Accordingly, the isotope fractionation factor (α) for the general isotope exchange
136 reaction between X and Y may be written as (Liu and Tossell, 2005):

137 $$\alpha = \frac{RPFR(X)}{RPFR^{\frac{1}{n}}(Y)} = \frac{\beta(X)}{\beta(Y)} \qquad \text{(Eq. 2)}$$

138 where the reduced isotopic partition function ratio (β factor) of X and Y is given by:

139 $$\beta = \frac{Q^*}{Q} = \prod_{i}^{3N} \frac{u_i^*}{u_i} \frac{\exp(-\frac{u_i^*}{2})}{1-\exp(-u_i^*)} \frac{1-\exp(-u_i)}{\exp(-\frac{u_i}{2})} \qquad \text{(Eq. 3)}$$

140 and Q is the vibrational partition function, the asterisk refers to the heavy isotope, *N* is the number of
141 atoms in the unit cell, and subscript *i* is the vibration mode order number. The term of u_i (u^*_i) is
142 calculated using the relationship:

143 $$u_i = \frac{hc \cdot v_i}{kT} \qquad \text{(Eq. 4)}$$

144 where *h* is Plank's constant, *c* is the speed of light, v_i is the vibration frequency of the i^{th} mode, *k* is
145 the Boltzmann's constant and *T* is the temperature in degrees Kelvin.

146 The isotopic composition of chlorine is expressed as per mil deviations from the Standard Mid-
147 Ocean Chloride isotopic composition (SMOC):

148 $$\delta^{37}Cl = \left(\frac{(^{37}Cl/^{35}Cl)_{sample}}{(^{37}Cl/^{35}Cl)_{SMOC}} - 1\right) \times 10^3 \qquad \text{(Eq. 5)}$$

149 The relationship of the chlorine isotope fractionation factor ($\alpha_{mineral\text{-}fluid}$) between chlorine-bearing
150 minerals and fluid and the extent of chlorine isotope fractionation between these phases ($\Delta_{mineral\text{-}fluid}$)
151 is expressed by Eq. 6.

Liu, X., Wei, H.-Z., Williams-Jones, A., Ma, J., Lu, J.-J., Jiang, S.-Y., Li, Y.-C., and Dong, G., 2021,
Chlorine isotope fractionation during serpentinization and hydrothermal mineralization: A density functional theory study:
Chemical Geology, v. 581, p. 120406.

$$1000ln\alpha_{mineral\text{-}fluid} \cong \delta^{37}Cl_{mineral}\text{-}\delta^{37}Cl_{fluid} = \Delta_{mineral\text{-}fluid} \quad \text{(Eq. 6)}$$

2.2. Models of minerals

In this work, the common chlorine-bearing minerals for which the reduced isotopic partition function ratio for $^{37}Cl/^{35}Cl$ (i.e., β-factors) is calculated are: apatite ($Ca_5(PO_4)_3(F,Cl,OH)$); muscovite ($KAl_2(Si_3Al)O_{10}(OH)Cl$); phlogopite ($KMg_3(Si_3Al)O_{10}(OH)Cl$); tremolite ($Ca_2Mg_5Si_8O_{22}(OH)Cl$); lizardite ($Mg_3Si_2O_5(OH,Cl)_4$); marialite ($Na_4Al_3Si_9O_{24}Cl$) and halite (NaCl). The generalized-gradient approximation (GGA) method together with the exchange-correlation functional of Perdew, Burke and Ernzerhof (PBE) (Perdew et al., 1996), and norm-conserving pseudopotentials were employed in both geometric optimizations and phonon calculations in the PBC model for the chlorine-bearing minerals. The calculations were carried out using the Cambridge Serial Total Energy Software Package (CASTEP) (Clark et al., 2005). Illustrations of the mineral models are available in our recent paper (Liu et al., 2021) and provided in the Appendix (Fig. S1).

2.3. Models for aqueous fluids

2.3.1 A Model for the serpentinizing fluid

Considering that in aqueous fluids (e.g., seawater) chloride ions interact electrically with shells of uniformly distributed H_2O dipoles, an electrostatic model of a $Cl^-(H_2O)_n$ cluster (n = 6 - 8) composed of two shells of dipoles (H_2O molecules) was employed to model serpentinization (the alteration of the oceanic lithospheric mantle by seawater). The β-factors of the hydrated chloride have been calculated (Czarnacki and Halas, 2012) and were used to compute the β-factors for the serpentinizing fluids in this study (see below).

2.3.2 ab initio molecular dynamic simulation of ore-forming fluids in hydrothermal systems

Numerous experimental and theoretical studies of high temperature aqueous speciation and the modelling of hydrothermal mineralization have demonstrated that a large number of ore metals, including Fe, Cu, Zn, Pb, Sn, Ag and the REE, are transported to the sites of deposition as chloride

Liu, X., Wei, H.-Z., Williams-Jones, A., Ma, J., Lu, J.-J., Jiang, S.-Y., Li, Y.-C., and Dong, G., 2021,
Chlorine isotope fractionation during serpentinization and hydrothermal mineralization: A density functional theory study:
Chemical Geology, v. 581, p. 120406.

complexes (e.g., Liu et al., 2007; Heinrich and Seward, 1990; Testemale et al., 2009; Seward et al., 2014; Williams-Jones and Migdisov, 2014). Thus, if we are to model Cl-isotopic fractionation between minerals and ore-forming fluids, it is necessary to consider the role of Cl complexes of these metals in this fractionation. As a first approximation, however, we can restrict the list of metal complexes to those of Fe, because in most ore fluids, the proportions of the other metals are small relative to that of Fe. Indeed, fluid inclusion studies have shown that, in many ore-forming fluids, the concentration of Fe approaches that of Na, the main metal in most hydrothermal fluids (e.g., Bodnar et al., 2014). Testemale et al. (2009) summarized the available information on Fe(II) chloro-complexes in acidic high temperature Cl-rich aqueous solutions and emphasized the importance of high-order chloro-complexes for this transport. In general, complexes with higher ligand number increase in abundance as the chloride activity increases (Sharps et al., 1993; Gammons et al., 1997; Xiao et al., 1998; Hill et al., 2010; Seward et al., 2014). At ambient temperature, the main Fe species are hydrated Fe^{2+}, $FeCl^{+}$, and $FeCl_2$ (e.g., Heinrich and Seward, 1990; Zhao and Pan, 2001; Liu et al., 2007), whereas at high temperature $FeCl_2$ and $FeCl_4^{2-}$ are the principal Fe species, with $FeCl_4^{2-}$ dominating at high salinity (Zhao and Pan, 2001; Liu et al., 2007; Hill et al., 2010). A study of the solubility and speciation of iron at hydrothermal conditions using synchrotron-radiation micro-XRF, XANES analyses and Raman spectroscopy has shown that the octahedral complexes $FeCl_x(H_2O)_{6-x}^{2-x}$ (x = 0 - 3) are the dominant Fe(II) species at lower Cl-Fe ratios, and that the tetrahedral complexes $FeCl_4^{2-}$ or $FeCl_3(H_2O)^{-}$ dominates at high Cl-Fe ratios (Scholten et al., 2019).

To quantitatively assess the effects of different configurations of aqueous metal-chloride complexes on the β-factors for an ore-forming hydrothermal fluid with both low Cl/Fe and high Cl/Fe ratios, we carried out *ab initio* molecular dynamic simulations (AIMD) to determine the stable speciation of iron at hydrothermal conditions. The AIMD was carried out with the PBE functional together with norm-conserving pseudopotentials using the CASTEP module in the Materials Studio software package (Accelrys Inc., version 7.0). The aqueous solution was surrounded by a

Liu, X., Wei, H.-Z., Williams-Jones, A., Ma, J., Lu, J.-J., Jiang, S.-Y., Li, Y.-C., and Dong, G., 2021,
Chlorine isotope fractionation during serpentinization and hydrothermal mineralization: A density functional theory study:
Chemical Geology, v. 581, p. 120406.

periodically repeated box that contained one Na_2FeCl_4 or one $FeCl_2$ surrounded by 40 water molecules. With optimization, the Na_2FeCl_4 species transformed to an octahedron of $Na_2FeCl_4(H_2O)_2$ from a tetrahedral structure. All MD simulations were performed in the NVT ensemble for 573.15 K with a trajectory longer than > 30 ps and an integration step of 0.5 fs. The intramolecular Fe-Cl bond lengths of aqueous Na_2FeCl_4 and $FeCl_2(H_2O)_4$ in 30 - 40 ps of MD simulation trajectory were compared and the difference in the randomly selected configuration was used to check the convergence of the MD simulation on the conformational distribution. Finally, twenty representative configurations of aqueous ferrous chloride complexes were extracted from each AIMD trajectory and examined.

2.4 Error estimation

The calculation accuracy of β-factor values in minerals depends primarily on two factors, the uncertainty associated with the calculated phonon frequencies between isotopomers using density functional perturbation theory (DFPT) and the uncertainty related to anharmonic effects (Méheut et al., 2007). The uncertainty in the calculation of phonon frequencies by DFT, at the PBE level, leads to a systematic relative error of about 5%, which is similar to that affecting the calculation of β-factors. The uncertainty arising from anharmonic effects in minerals is relatively small (Méheut et al., 2007). The relative error associated with the calculation of the phonon frequency in this study is estimated to be ± 4%, which is similar to that reported by Méheut et al. (2007). Consequently, the relative error for the β factor of the minerals is estimated to be ± 4%.

The errors in the β-factor calculation for fluids are relatively large due to instantaneous weak interactions among ions and molecules in aqueous solution (e.g., van der Waals forces and hydration effects). They were estimated from the vibrational frequencies calculated for individual configurations generated by the 30 ps of AIMD trajectories. The standard deviation of the calculated β factor from the selected configurations along the AIMD trajectories of the two fluids was estimated

Liu, X., Wei, H.-Z., Williams-Jones, A., Ma, J., Lu, J.-J., Jiang, S.-Y., Li, Y.-C., and Dong, G., 2021,
Chlorine isotope fractionation during serpentinization and hydrothermal mineralization: A density functional theory study:
Chemical Geology, v. 581, p. 120406.

to be 8.6%. The overall absolute errors in $\Delta^{37}Cl_{mineral\text{-}fluid}$ estimated by the error propagation are ± 0.20‰ for low temperature (i.e., 373.15 K) and ± 0.09‰ for high temperature (i.e., 573.15 K).

3. RESULTS

3.1. Calculation of RPFRs of hydrated chloride in serpentinizing fluids

The β-factors for hydrated chloride as a function of temperature have been calculated by Czarnacki and Halas (2012) (Fig. 1). Based on the experimental results of Eggenkamp et al. (1995), Schauble et al. (2003) estimated values of 2.1 - 3.0‰ for $1000ln\beta_{brine}$ and a value of +0.26‰ for $\Delta^{37}Cl_{halite\text{-}aqueous\ Cl}$ at 295 K, which is less than the 1000lnβ value of 3.13‰ for aqueous chloride calculated by Czarnacki and Halas (2012). The 1000lnβ values calculated by Czarnacki and Halas (2012) were therefore corrected in this work, using the expression $\Delta 1000ln\beta = (-0.58)\times(\frac{295}{T})^2‰$, assuming that $1000ln\beta \propto T^{-2}$ and the difference of Δ1000lnβ between the calculations of Schauble et al. (2003) and Czarnacki and Halas (2012) is -0.58‰ at 295 K, as shown in Fig. 1.

Liu, X., Wei, H.-Z., Williams-Jones, A., Ma, J., Lu, J.-J., Jiang, S.-Y., Li, Y.-C., and Dong, G., 2021,
Chlorine isotope fractionation during serpentinization and hydrothermal mineralization: A density functional theory study:
Chemical Geology, v. 581, p. 120406.

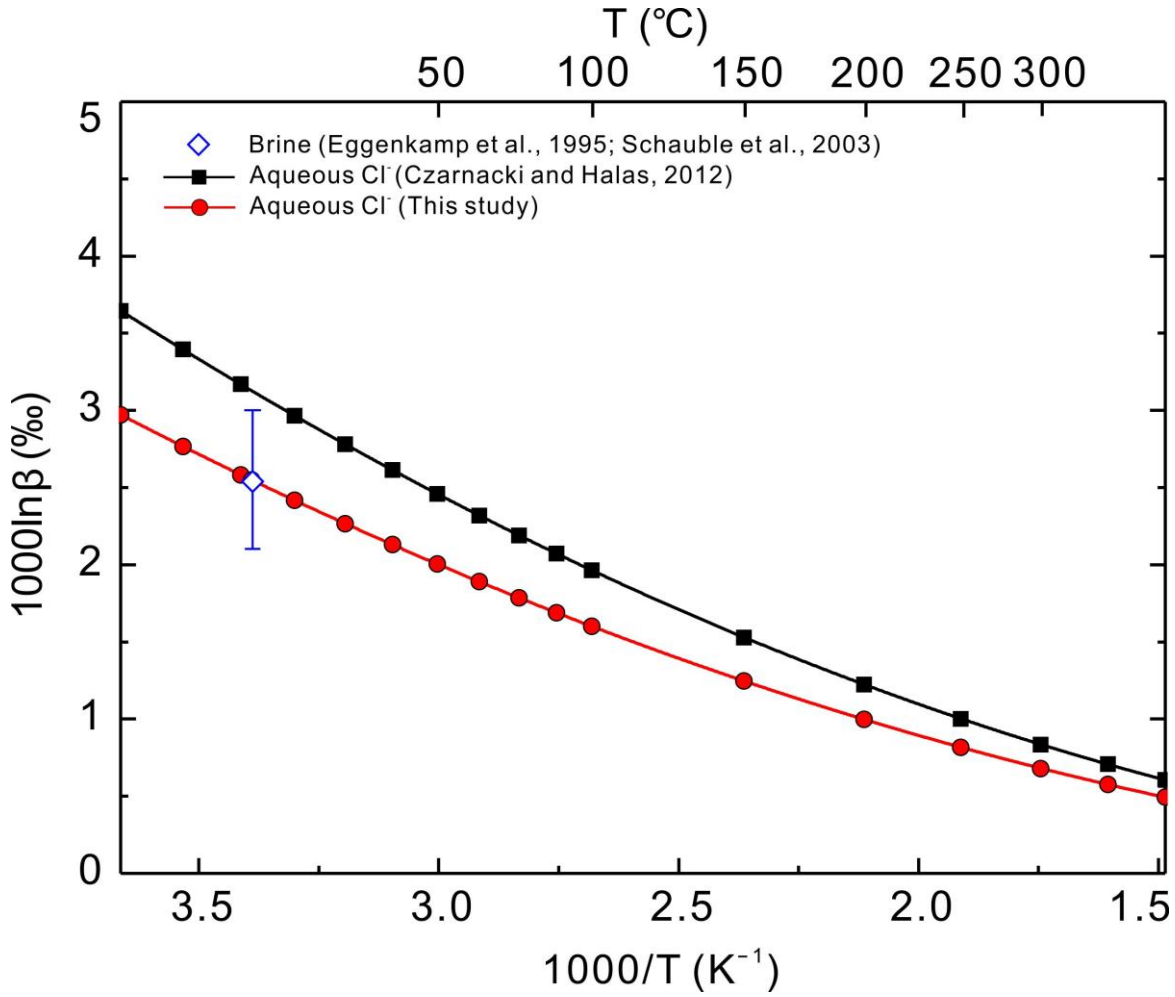

Fig. 1. Reduced partition function ratios 1000lnβ for aqueous chloride as a function of temperature. The red line corresponds to the corrected 1000lnβ vales for aqueous chloride, based on the original theoretical data (black line) from Czarnacki and Halas (2012). The vertical bar indicates the values of 1000lnβ for brine at 295 K estimated by Schauble et al. (2003) on the basis of experimental data from Eggenkamp et al. (1995).

3.2. AIMD trajectory of iron(II) chlorocomplexes in ore-forming fluids

Peaks in the first radial distribution function of Fe-O ($RDF_{Fe\text{-}O}$) and Fe-Cl ($RDF_{Fe\text{-}Cl}$) for $FeCl_2(H_2O)_4$-$36H_2O$ fluid at 573.15 K and 400 MPa are in the range of 1 Å - 3 Å, and are centered at ~1.95 Å and ~2.35 Å (Fig. 2ab). These peaks correspond to about 4.0 on the running CN (coordination number) curve, indicating a 4-fold O coordination and 2-fold Cl coordination. In $Na_2FeCl_4(H_2O)_2$-$38H_2O$-bearing fluid, the first $RDF_{Fe\text{-}O}$ and $RDF_{Fe\text{-}Cl}$ peaks are shifted slightly

Liu, X., Wei, H.-Z., Williams-Jones, A., Ma, J., Lu, J.-J., Jiang, S.-Y., Li, Y.-C., and Dong, G., 2021,
Chlorine isotope fractionation during serpentinization and hydrothermal mineralization: A density functional theory study:
Chemical Geology, v. 581, p. 120406.

upward to 2.05 Å and downward to 2.25 Å, respectively, and on the CN curve they correspond to values of approximately 2.0 and 4.0, respectively (Fig. 2cd). The simulation results suggest that the hydration shells of Fe^{2+} are very flexible. The intramolecular Fe-O and Fe-Cl bond lengths of aqueous $FeCl_2(H_2O)_4$ and $Na_2FeCl_4(H_2O)_2$ in the 30 ps MD simulation trajectory are compared in Figure 3. The variable Fe-O and Fe-Cl distances along the trajectories of Figure 3 show the ligand exchange at the timescale of picoseconds. The narrow variation ranges in Fe-O and Fe-Cl bond distances of two aqueous species along the long simulation trajectories ensure the convergence of the MD simulation of the conformational distribution. As a result, twenty representative configurations of fluid extracted from each of the AIMD trajectories were shown to be uncorrelated (Fig. S2). These were used to compute the RPFRs of two iron(II) chlorocomplexes in ore-forming fluids.

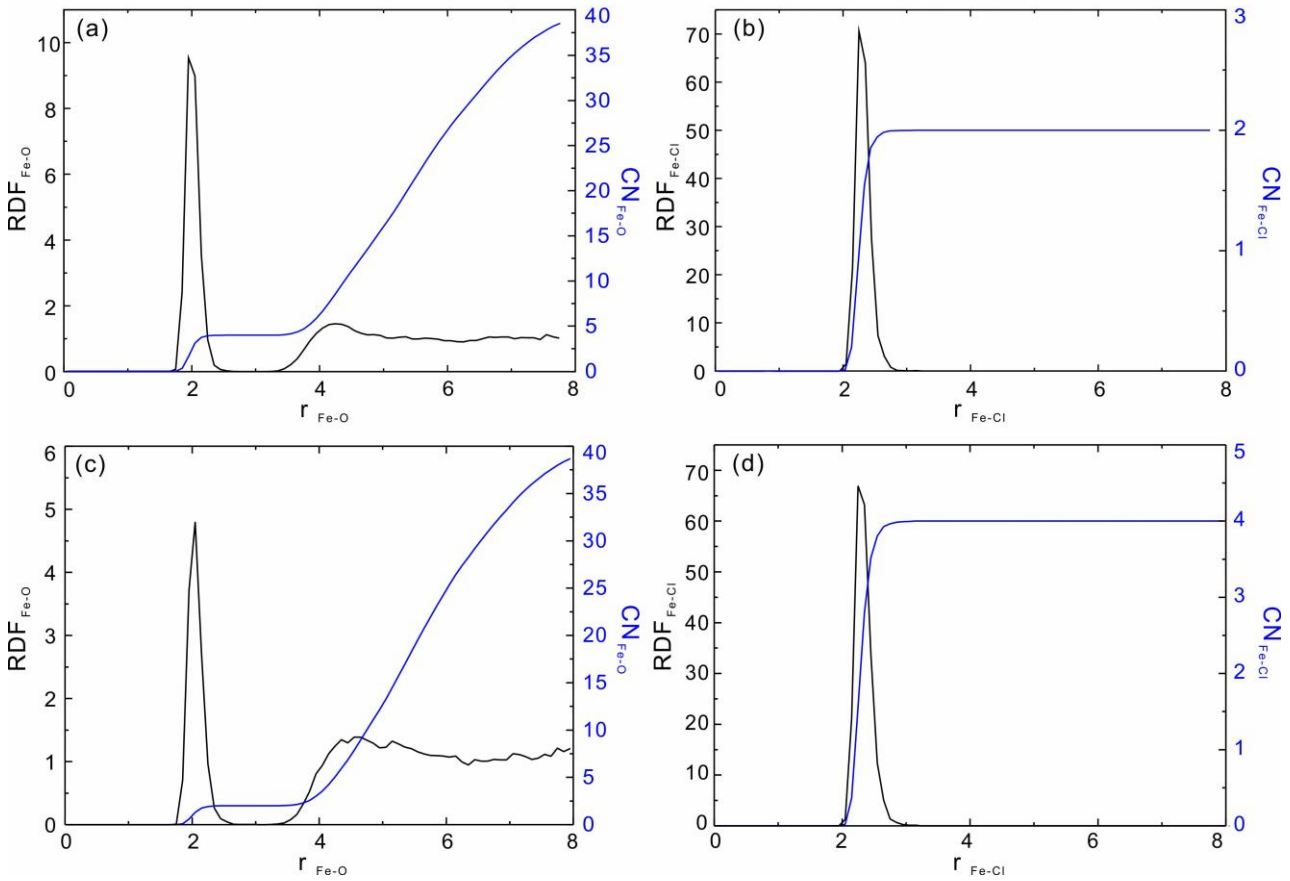

Fig. 2. The radial distribution functions (RDFs) and running coordination numbers (CNs) for O and Cl around Fe^{2+} cations. (a) and (b) show $RDF_{Fe\text{-}O}$, $CN_{Fe\text{-}O}$ and $RDF_{Fe\text{-}Cl}$, $CN_{Fe\text{-}Cl}$ for

Liu, X., Wei, H.-Z., Williams-Jones, A., Ma, J., Lu, J.-J., Jiang, S.-Y., Li, Y.-C., and Dong, G., 2021,
Chlorine isotope fractionation during serpentinization and hydrothermal mineralization: A density functional theory study:
Chemical Geology, v. 581, p. 120406.

$FeCl_2(H_2O)_4 \cdot 36H_2O$; (c) and (d) show $RDF_{Fe\text{-}O}$, $CN_{Fe\text{-}O}$ and $RDF_{Fe\text{-}Cl}$, $CN_{Fe\text{-}Cl}$ for $Na_2FeCl_4(H_2O)_2 \cdot 38H_2O$.

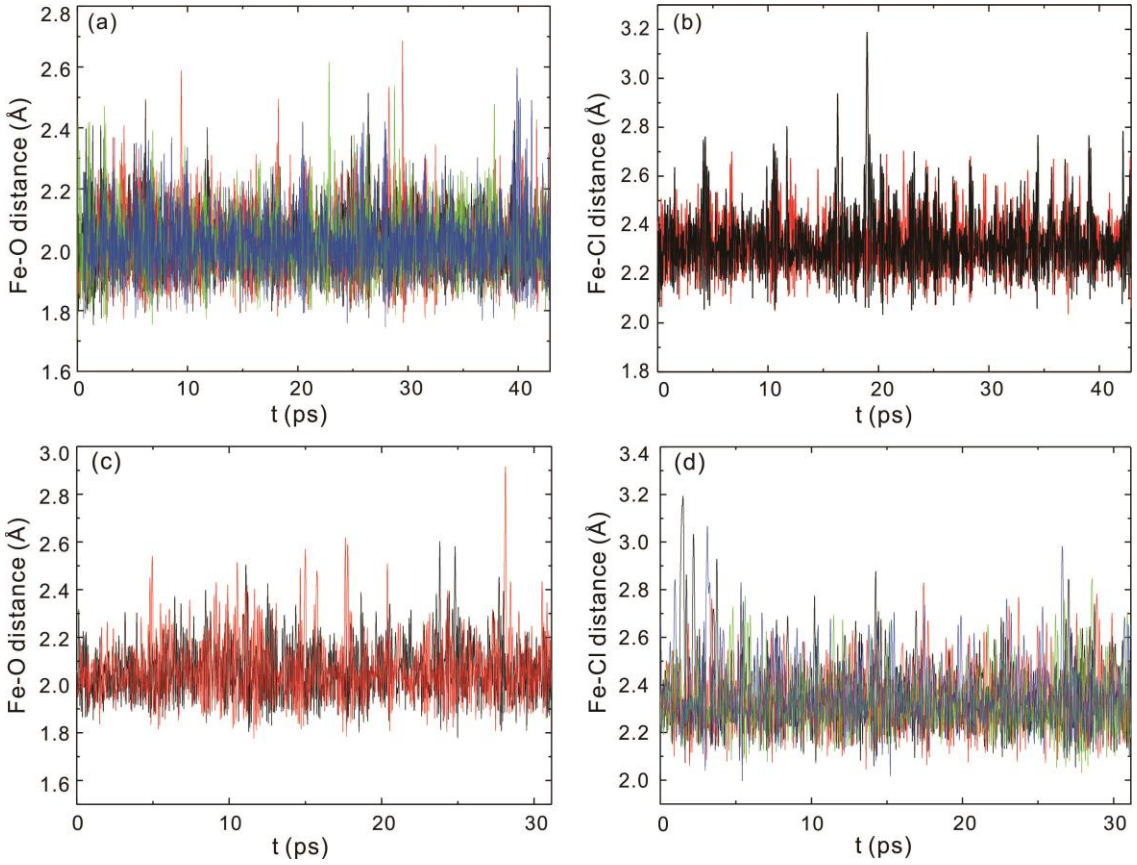

Fig. 3. Variations in Fe-O and Fe-Cl distances along the AIMD trajectories. (a) and (b) show Fe-O and Fe-Cl distances in $FeCl_2(H_2O)_4 \cdot 36H_2O$, respectively; (c) and (d) show Fe-O and Fe-Cl distances in $Na_2FeCl_4(H_2O)_2 \cdot 38H_2O$, respectively. The distances of two Fe-Cl bonds and four Fe-O bonds in $FeCl_2(H_2O)_4 \cdot 36H_2O$ and these of four Fe-Cl bonds and two Fe-O bonds in $Na_2FeCl_4(H_2O)_2 \cdot 38H_2O$ are presented with different colors.

3.2. Calculation of RPFRs of iron(II) chlorocomplexes in ore-forming fluids

In a mineral-fluid system, the level of computational treatment of the aqueous environment is more important than the treatment of the mineral environment in determining the overall quality of the predicted mineral-aqueous isotope fractionation (Rustad et al., 2010). The RPFRs were computed on twenty configurations extracted along the AIMD trajectories, and the average 1000lnβ of

Liu, X., Wei, H.-Z., Williams-Jones, A., Ma, J., Lu, J.-J., Jiang, S.-Y., Li, Y.-C., and Dong, G., 2021,
Chlorine isotope fractionation during serpentinization and hydrothermal mineralization: A density functional theory study:
Chemical Geology, v. 581, p. 120406.

$FeCl_2(H_2O)_4$-$36H_2O$ fluid and $Na_2FeCl_4(H_2O)_2$-$38H_2O$ fluid at 573.15 K, 400 MPa were determined to be 1.2323 ± 0.1046 and 1.2409 ± 0.0852 (Fig. 4a, b). To assess the influence of coordination bond on the reduced isotopic partition function ratios in the individual configurations of aqueous chlorine-bearing solutions, we compared the relationship of 1000lnβ to the Fe-Cl length (Fig. 4c, d). The strong negative correlation between the 1000lnβ values and the Fe-Cl bond length in the two aqueous Fe-chloride species, confirms the importance of the coordination bonds in the first hydration shell on chlorine isotope fractionation in fluids.

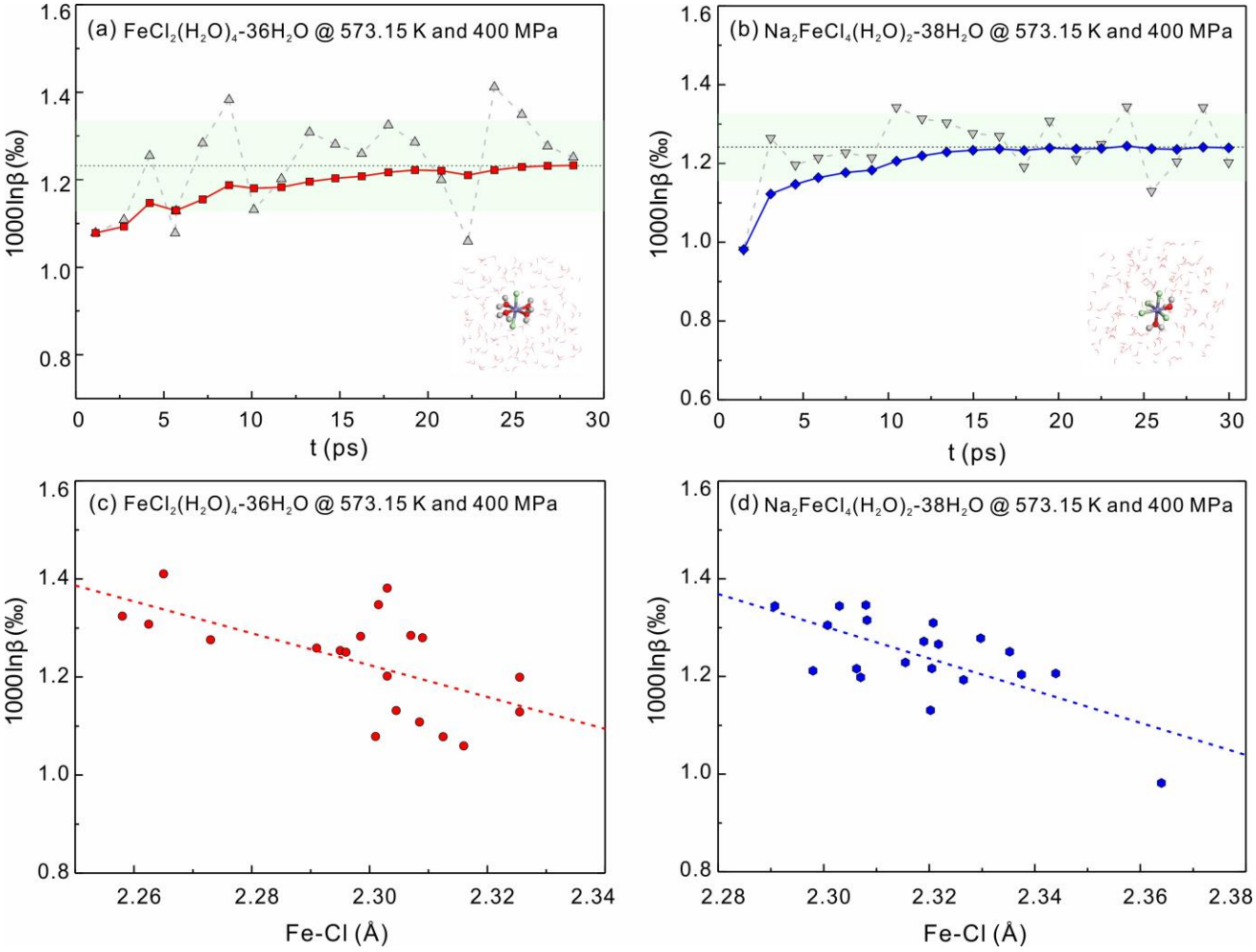

Fig. 4. Individual β values (1000lnβ) of selected configurations (colored solid points) for $FeCl_2(H_2O)_4 \cdot 36H_2O$ (a), $Na_2FeCl_4(H_2O)_2 \cdot 38H_2O$ (b) and their cumulative averages (gray hollow points) in the time frame. The inserts are the representative configurations of $FeCl_2(H_2O)_4 \cdot 36H_2O$ and $Na_2FeCl_4(H_2O)_2 \cdot 38H_2O$ extracted from AIMD trajectories; (c) and (d) show the relationship

Liu, X., Wei, H.-Z., Williams-Jones, A., Ma, J., Lu, J.-J., Jiang, S.-Y., Li, Y.-C., and Dong, G., 2021,
Chlorine isotope fractionation during serpentinization and hydrothermal mineralization: A density functional theory study:
Chemical Geology, v. 581, p. 120406.

293 between 1000lnβ and Fe-Cl length in the $FeCl_2(H_2O)_4 \cdot 36H_2O$- and $Na_2FeCl_4(H_2O)_2 \cdot 38H_2O$-bearing
294 aqueous fluid systems

295

296 ## 4. DISCUSSION

297 Subduction zones play a major role in the cycling of elements in the Earth, transferring material
298 from the crust to the mantle. Chlorine isotopes and their fractionation provide a valuable means of
299 tracing the paths of these elements during subduction. In evaluating Cl isotope fractionation,
300 however, it is important to recognize that the fractionation occurs in several steps. Thus, the down-
301 going slab (oceanic crust and mantle) is first altered by seawater at a spreading center, adding
302 chlorine to the slab. During subduction, these altered rocks, which include serpentinite, undergo
303 metamorphic dehydration and partial melting at forearc to subarc depths, releasing Cl-bearing fluids
304 for serpentinization of the mantle wedge. Partial melting of the wedge produces arc magmas that
305 ascend to shallow crustal levels, where they exsolve hydrothermal fluids (Fig. 5). These fluids are
306 enriched in chloride and transitional metal ions which leads to the formation of stable metal-chloride
307 complexes, yielding metal concentrations that are in some cases sufficient to form magmatic-
308 hydrothermal ore deposits. The Cl isotope fractionation occurring at the different steps referred to
309 above is discussed below.

310

Liu, X., Wei, H.-Z., Williams-Jones, A., Ma, J., Lu, J.-J., Jiang, S.-Y., Li, Y.-C., and Dong, G., 2021,
Chlorine isotope fractionation during serpentinization and hydrothermal mineralization: A density functional theory study:
Chemical Geology, v. 581, p. 120406.

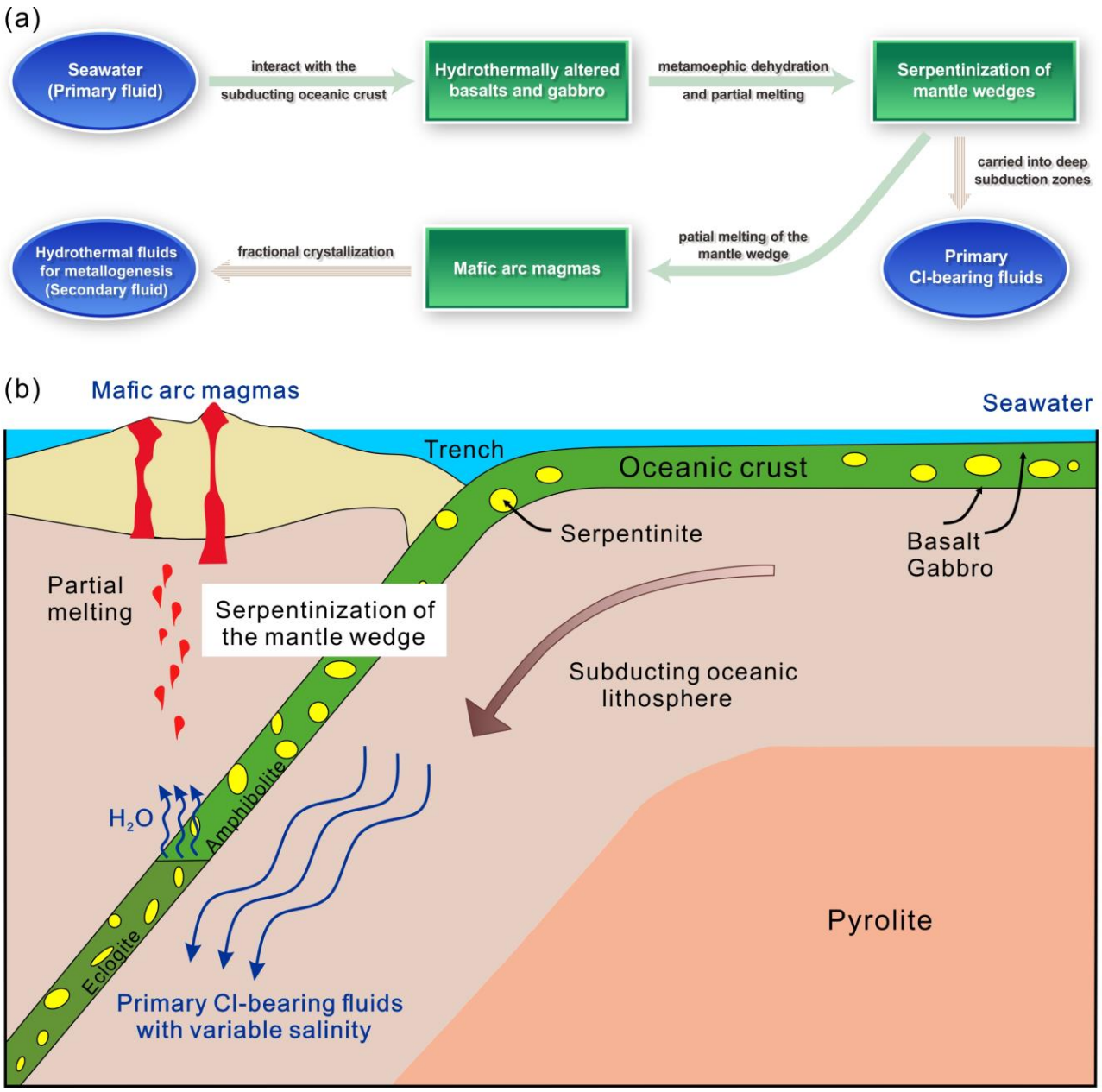

Fig. 5. (a) A schematic diagram illustrating the path of fluid evolution through a subduction zone from its introduction as seawater to its final exsolution as an ore-forming hydrothermal fluid. (b) A cartoon showing the subduction of oceanic lithosphere and the path of fluid evolution in this setting (modified from Ringwood, 1974).

4.1. Influence of the configuration of iron-chloride complexes on the RPFRs in ore-forming fluids

Aqueous metal speciation plays an important role in controlling metal transport and deposition in hydrothermal fluids (Seward and Driesner, 2004; Brugger et al., 2010; Williams-Jones and Migdisov,

Liu, X., Wei, H.-Z., Williams-Jones, A., Ma, J., Lu, J.-J., Jiang, S.-Y., Li, Y.-C., and Dong, G., 2021,
Chlorine isotope fractionation during serpentinization and hydrothermal mineralization: A density functional theory study:
Chemical Geology, v. 581, p. 120406.

2014; Mei et al., 2015). Most commonly, the metals are transported as metal-chloride complexes (Seward et al., 2014). The AIMD simulation showed that under hydrothermal conditions (573.15 K and 400 MPa), Fe(II) chlorocomplexes have their highest stability in octahedral configuration. This contradicts a previous study, which concluded that Fe(II) - chloride complexes gradually transform from octahedrally to tetrahedrally coordinated configurations at temperatures between 10 to 100℃ and chloride concentrations from 0.1 to 16 mol·kg^{-1} (Zhao and Pan, 2001). Numerous experimental studies have shown that a variety of factors may affect the coordination of metal-chloride complexes (e.g., temperature, salinity, pH, redox state and pressure), and therefore affect the mobility of metals in hydrothermal systems (Brugger et al., 2016 and references therein). For example, the solubility of Fe-bearing minerals is controlled by octahedral - tetrahedral phase transitions (Brugger et al., 2016). Increased pressure facilitates the transition from tetrahedral to octahedral structures as observed in Co(II)-chloride complexes and Ni(II)-chloride complexes (Lüdemann and Franck, 1967; Suleimenov, 2004; Brugger et al., 2016). In addition, it has been proposed that the configuration would also be affected by variable Cl-Fe ratios, in which octahedral $FeCl_x(H_2O)_{6-x}^{2-x}$ (x = 0 - 3) is the main configuration at low Cl/Fe ratios, and tetrahedral $FeCl_4^{2-}$ or $FeCl_3(H_2O)^-$ is the main configuration at high Cl/Fe ratios (Scholten et al., 2019).

It has been recognized that the first hydration shell (e.g., coordination configuration, and coordination number) may affect the physicochemical properties of hydrated ions (or molecules) by shifting vibrational frequencies and consequently inducing isotope fractionation (e.g., Pye and Rudolph, 2001; Kubicki, 2001; Zhou et al., 2006; Vchirawongkwin and Rode, 2007; Miller et al., 2007; Rustad and Bylaska, 2007; Rustad et al., 2008; Pinilla et al., 2015; Kowalski and Jahn, 2011; Dupuis et al., 2015; Li et al., 2020, 2021). During the AIMD simulation of the secondary fluids containing Fe(II) - chloride complexes with low and high Cl/Fe ratios, both H_2O and the chloride ion operated as the chelating ligands for coordinating with Fe(II), and stabilized as the octahedral configurations $FeCl_2(H_2O)_4$ and $Na_2FeCl_4(H_2O)_2$, respectively. There is a minor difference in the

Liu, X., Wei, H.-Z., Williams-Jones, A., Ma, J., Lu, J.-J., Jiang, S.-Y., Li, Y.-C., and Dong, G., 2021,
Chlorine isotope fractionation during serpentinization and hydrothermal mineralization: A density functional theory study:
Chemical Geology, v. 581, p. 120406.

reduced isotopic partition function ratio (β-factor) for the two Fe(II) chloro-complexes in hydrothermal ore-forming fluids as temperature increases from 373.15 K to 1173.15 K (Fig. 6). The near coincidence of the two curves indicates that the effect of the hydration number in the first hydration shell on the chlorine isotope fractionation of iron(II) chloro-complexes is too small to be distinguished. In a future study, we will investigate the effect of coordination configuration and coordination number on the chlorine isotope fractionation for other transitional metal-chloride complexes in ore-forming fluids, e.g., zinc/copper chloro-complexes.

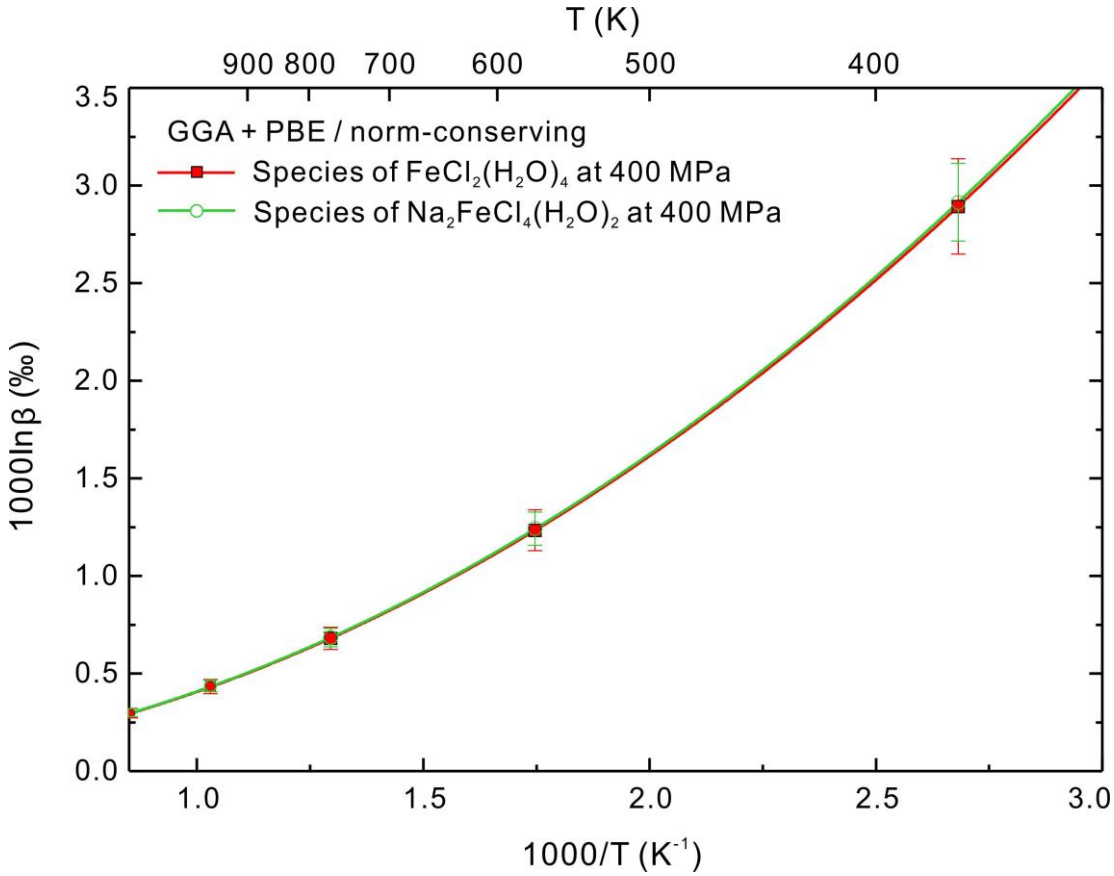

Fig. 6. Values of 1000lnβ versus 1000/T for $^{37}Cl/^{35}Cl$ for Fe(II) chloride species in a hydrothermal ore-forming fluid.

4.2. Equilibrium chlorine isotope fractionation between minerals and fluid during hydrothermal ore-formation

Liu, X., Wei, H.-Z., Williams-Jones, A., Ma, J., Lu, J.-J., Jiang, S.-Y., Li, Y.-C., and Dong, G., 2021,
Chlorine isotope fractionation during serpentinization and hydrothermal mineralization: A density functional theory study:
Chemical Geology, v. 581, p. 120406.

The Br/Cl ratios and $\delta^{37}Cl$ values of evaporites (e.g., halite) enable discrimination of different types of basinal brines and their relationship to mineralization (Eastoe and Guilbert, 1992; Zhao et al., 2021). Their application, however, is much broader. Indeed, these parameters of fluid inclusions are commonly used to distinguish a variety of saline fluid types including those of magmatic origin (e.g., Banks et al., 2000; Lüders et al., 2002; Chiaradia et al., 2006; Gleeson and Smith, 2009; Eggenkamp, 2014; Bernal, 2015; Bénard et al., 2020), as well as to constrain mineralization stages (e.g. Eastoe et al., 1989; Hanley et al., 2011). It is, nevertheless, important to note that the original $\delta^{37}Cl$ signatures of the fluids may have changed as a result of kinetic isotope fractionation during phase separation, condensation, and/or mixing at, or near, the site of mineralization (Nahnybida et al., 2009).

Using the calculated $1000\ln\beta$ of chlorine-bearing minerals (Table S1), we have estimated the temperature dependence of chlorine isotope fractionation between chlorine-bearing minerals and hydrothermal ore-forming fluids containing iron chlorocomplexes (Fig. 7). The chlorine isotope fractionation factors $\Delta^{37}Cl_{\text{minerals-hydrothermal fluid}}$ vary in a wide range (e.g., from -0.85 to +0.95‰ at 573.15 K and 400 MPa). Several minerals, notably phlogopite, and tremolite, prefer the heavy isotope, ^{37}Cl, whereas other minerals (e.g., marialite and halite) prefer the lighter isotope, ^{35}Cl, relative to the hydrothermal ore-forming fluid. The apparently significant chlorine isotope fractionation during mineral precipitation (e.g., phlogopite, tremolite, marialite and halite) may partly reflect the large variation of $\delta^{37}Cl$ observed in fluid inclusions in the same geological setting (Eastoe et al., 1989; Gleeson and Smith, 2009; Richard et al., 2011). In contrast, the chlorine isotope fractionation between apatite-group minerals and hydrothermal ore-forming fluids is relatively small, ranging from 0.06 to 0.69‰ at typical hydrothermal conditions. Therefore, we suggest that apatite-group minerals (common accessory minerals in ore deposits) might be an alternative to fluid inclusions for constraining the origin and evolution of hydrothermal fluids using $\delta^{37}Cl$ values.

Liu, X., Wei, H.-Z., Williams-Jones, A., Ma, J., Lu, J.-J., Jiang, S.-Y., Li, Y.-C., and Dong, G., 2021,
Chlorine isotope fractionation during serpentinization and hydrothermal mineralization: A density functional theory study:
Chemical Geology, v. 581, p. 120406.

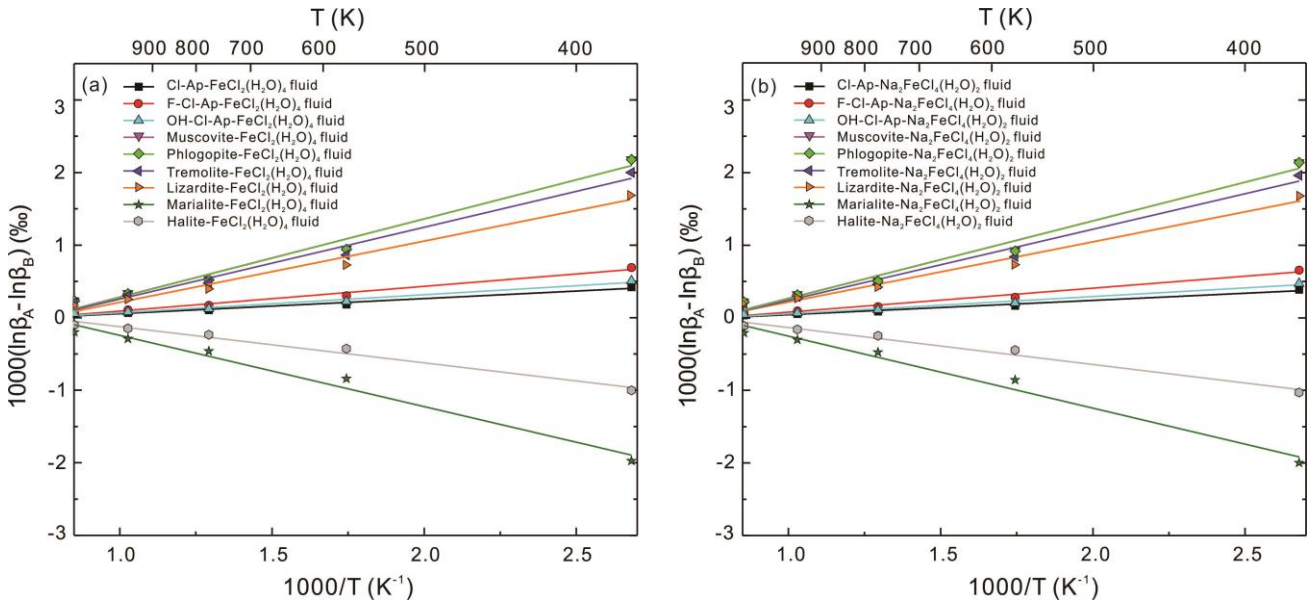

Fig. 7. The equilibrium chlorine isotope fractionation of various chlorine-bearing minerals with a hydrothermal ore-forming fluid containing $FeCl_2(H_2O)_4 \cdot 36H_2O$ (a) and with a hydrothermal ore-forming fluid containing $Na_2FeCl_4(H_2O)_2 \cdot 38H_2O$ fluid (b).

4.3 Equilibrium chlorine isotope fractionation between minerals and fluid during serpentinization

Chlorine is an abundant anion in seawater, in most crustal fluids, and in fluids serpentinizing the mantle wedge in subduction zones (e.g., Kent et al., 2002; Manning, 2004; Scambelluri and Philippot, 2001; Stolper and Newman, 1994; Yardley, 1997; John et al., 2011). Hydrous minerals, such as serpentine, talc, chlorite, and amphibole, which have relatively high Cl concentrations, become enriched in ^{37}Cl during such fluid-rock interaction (Schauble et al., 2003; Wei et al., 2008).

Serpentinization, the alteration of ultramafic rocks (typically peridotite and komatiite) at relatively low temperature (≤ 500 ℃), produces serpentine minerals, (±) brucite, (±) talc, and (±) magnetite containing high concentrations of fluid-mobile elements (e.g., Ba, Cs, and Cl) (Huang et al., 2017). In addition, serpentine is the most important solid reservoir for volatile Cl and H_2O in the subducting slab and the mantle wedge (Wei et al., 2008). During subduction, serpentine is a particularly fertile source of water and Cl (Ruepke et al., 2002; Scambelluri et al., 1995; Thompson,

Liu, X., Wei, H.-Z., Williams-Jones, A., Ma, J., Lu, J.-J., Jiang, S.-Y., Li, Y.-C., and Dong, G., 2021,
Chlorine isotope fractionation during serpentinization and hydrothermal mineralization: A density functional theory study:
Chemical Geology, v. 581, p. 120406.

399 1992; Ulmer and Trommsdorff, 1995; Wei et al., 2008). Moreover, the dehydration of serpentine
400 minerals produces chlorine-rich fluids that may be linked to the genesis of arc magmas (Huang et al.,
401 2017). Serpentinization occurs in a variety of tectonic settings, including the ocean floor, mid-ocean
402 ridges, and subduction zones (e.g., Charlou et al., 1996, 2000; Maekawa et al., 2001; Hyndman and
403 Peacock, 2003; Mével, 2003; Evans et al., 2013). At slow spreading ridges, the deep penetration of
404 hydrothermally driven seawater along normal faults facilitates reaction of this water with mantle
405 peridotites and, thus, the formation of serpentinites, whereas at fast spreading ridges, where the
406 circulation of hydrothermally driven seawater occurs above the peridotites, there is an absence of
407 serpentinization (Chaussidon and Jambon, 1984; Shirodkar et al., 2014). Serpentinization leads to
408 important physical and chemical changes in the subducting lithosphere, which may provide a
409 geochemical pathways for recycling water-soluble trace elements into both the sub-arc region of
410 flux-melting and the deeper mantle, and may play an important role in the transfer of H_2O, chlorine,
411 and fluid-mobile elements into the mantle (Ranero et al., 2003; Huang et al., 2017). Serpentinite in
412 oceanic crust formed at slow spreading ridges contains significant amounts of chlorine and releases
413 large amounts of fluid during subduction, making it the main contributor of chlorine transferred to
414 the mantle during subduction (Carlson, 2001; Carlson and Miller, 1997; Christensen, 1978;
415 Scambelluri et al., 2001, 2004; Scambelluri and Philippot, 2001; Sharp and Barnes, 2004; Barnes et
416 al., 2006). It is also noteworthy that with progressive serpentinization, the seawater-derived fluids
417 (preserved as fluid inclusions) can attain high concentrations of chloride and bromide (Scambelluri et
418 al., 1997; Normand and Williams-Jones, 2007; Kawamoto et al., 2018).

419 The equilibrium fractionation of chlorine isotopes between minerals and fluid during
420 serpentinization was quantitatively evaluated in the current study for P-T conditions on the seafloor,
421 in the mantle wedge and in subduction zones. In so doing, we considered the fact that the chemical
422 and isotopic composition of the pore water is changed by chemical processes such as water-rock
423 interaction, salt dissolution and albitization as well as physical processes such as diffusion, ion

Liu, X., Wei, H.-Z., Williams-Jones, A., Ma, J., Lu, J.-J., Jiang, S.-Y., Li, Y.-C., and Dong, G., 2021,
Chlorine isotope fractionation during serpentinization and hydrothermal mineralization: A density functional theory study:
Chemical Geology, v. 581, p. 120406.

exchange and ion-filtration and the mixing of water bodies with different sources (Eggenkamp, 2014). A statistical analysis of chlorine isotope ratios for deep formation waters produces a mean $\delta^{37}Cl$ value of -0.37‰ (Eggenkamp, 2014). It is noteworthy, however, that sedimentary pore fluids have lower $\delta^{37}Cl$ values, ranging from -8.52 to +0.80‰, with the vast majority of the samples yielding negative values with an average of -2.03‰ (Ransom et al., 1995; Eastoe et al., 1999, 2001; Hesse et al., 2000; Lehmann et al., 2003; Zhang et al., 2007; Goden et al., 2004; Bonifacie et al., 2007; Agrinier et al., 2019, 2021).

The temperature-dependent equilibrium chlorine isotope fractionation factor (i.e., $1000\ln\alpha$) between serpentine (e.g., lizardite) and fluid was estimated for P-T conditions in the three geological settings of serpentinization referred to above, seafloor (abyssal serpentinites), mantle wedge and subduction zones. These estimates are illustrated in Figures 8a and 9 and discussed below.

(i) Abyssal serpentinites: The temperature range of abyssal serpentinization can vary from ~500 °C to that of the seafloor (near 0 °C) (Mével, 2003; Seyfried et al., 2004; Alt et al., 2007). For example, oxygen isotope data indicate that peridotites exposed by tectonic extension during opening of the Atlantic were serpentinized at relatively low temperature, at ~ 0 - 150 °C (Agrinier et al., 1996). The maximum pressure at which serpentinization occurs is reasonably well constrained by the geodynamic setting (Mével, 2003). This pressure for serpentinite formation in abyssal peridotites at mid-ocean ridges is ~ 0.3 GPa, and usually less than 0.2 GPa. Unfortunately, there is currently a lack of geobarometers with which to better constrain the pressure (Mével, 2003). Consequently, the theoretical estimate for $\Delta^{37}Cl_{serpentinite\text{-}fluid}$ is +0.49 to +4.46‰ and the $\delta^{37}Cl$ values are from -1.11 to +4.39‰ for serpentinites at the seafloor that are in isotopic equilibrium with seawater ($\delta^{37}Cl_{SMOC}$ of 0.0‰) or pore water ($\delta^{37}Cl_{pw}$ of -0.37‰, -2.03‰) (Fig. 8b). This satisfactorily explains the Gaussian nature of the $\delta^{37}Cl$ frequency distribution observed for abyssal serpentinites (e.g., Barnes et al., 2006; Wei et al., 2008) (Fig. 8c). The theoretical estimate is in good agreement with the observation that most seafloor serpentinites have slightly positive $\delta^{37}Cl$ values (~0.0 to + 0.5‰) due to interaction

Liu, X., Wei, H.-Z., Williams-Jones, A., Ma, J., Lu, J.-J., Jiang, S.-Y., Li, Y.-C., and Dong, G., 2021,
Chlorine isotope fractionation during serpentinization and hydrothermal mineralization: A density functional theory study:
Chemical Geology, v. 581, p. 120406.

with seawater which, in turn, is consistent with the similarity of the halogen composition of abyssal serpentinites (i.e., I/Cl and Br/Cl ratios) to that of seawater (Scambelluri et al., 2019). Some of these serpentinites have negative $\delta^{37}Cl$ values (down to - 1.6‰) due to their interaction with sediments and/or sedimentary pore water (Barnes and Sharp, 2006; Barnes et al., 2008, 2009; Bonifacie et al., 2008).

(ii) Forearc serpentinites in the mantle wedge: Serpentinization is widespread in the forearc mantle due to bending-related faulting of subducting oceanic lithosphere and infiltration of fluids from overlying sedimentary pore waters (Ranero et al., 2003). The I/Cl and Br/Cl ratios of forearc serpentinites are close to those of sedimentary pore fluids (i.e., Br/Cl of 10×10^{-3} mol/mol and I/Cl of 9×10^{-3} mol/mol), which is interpreted to reflect the involvement of sedimentary components in slab fluids released into the forearc mantle wedge during sediment compaction at shallow depths (Kendrick et al., 2013; Scambelluri et al., 2019). The temperature at the top and the bottom of the mantle wedge is about 650 - 750 °C, and above 1250 °C, respectively (Zheng et al., 2016; Zheng and Chen, 2016). Based on experimental determinations, the maximum temperature at which serpentine minerals are stable is 800°C (Scambelluri et al., 2019). Therefore, the temperature range over which serpentinites are present in the mantle wedge serpentinite is about 650 - 800 °C and the pressure range is ca. 1 - 5 GPa. Our estimate for the $\Delta^{37}Cl_{serpentinite\text{-}fluid}$ in the mantle wedge is +0.37 to +0.59‰, which, combined with the strongly negative $\delta^{37}Cl$ of pore water in marine sediments (-8.52 to +0.80‰; see above), leads to $\delta^{37}Cl$ values for forearc serpentinites of -1.4 to -1.6‰ (Fig. 9). These theoretical estimates agree well with the negative $\delta^{37}Cl$ values (down to -2.11‰) observed in serpentinites from ODP cores 173-1068A (Barnes and Sharp, 2006).

(iii) Subduction-zone serpentinites: The elemental compositions of most subduction-zone serpentinites can be difficult to decipher because of superposed stages of oceanic and subduction-related hydration (e.g., Cs/U relative to Rb/U, Peters et al., 2017; REE profiles, Scambelluri et al., 2019). During subduction, sediments and altered oceanic crust are progressively dehydrated and

Liu, X., Wei, H.-Z., Williams-Jones, A., Ma, J., Lu, J.-J., Jiang, S.-Y., Li, Y.-C., and Dong, G., 2021,
Chlorine isotope fractionation during serpentinization and hydrothermal mineralization: A density functional theory study:
Chemical Geology, v. 581, p. 120406.

interact with the subducted abyssal serpentinites and partially hydrated peridotites (e.g. Deschamps et al., 2012; van Keken et al., 2011). Serpentine minerals are generally considered to form at the subduction plate interface, a relatively thin layer, and the depth of this interface generally extends from about 20 to 140 km (Deschamps et al., 2013; Hilairet and Reynard, 2009; Schwartz et al., 2001; Kawakatsu and Watada, 2007). The pressure corresponding to this depth is about 0.3 - 5 GPa (Deschamps et al., 2013). Most of the subducted water is released from the slab and percolates through the mantle wedge (Deschamps et al., 2013). The temperature of the subducting slab is about 100 - 650 °C (Zheng and Chen, 2016). Assuming the isotope exchange reaches equilibrium, our theoretical estimate predicts a relatively large chlorine isotope fractionation, i.e., values of $\Delta^{37}Cl_{serpentinite\text{-}fluid}$ of +0.49 to +3.57‰ (Fig. 9). These values are consistent with the observation of high $\delta^{37}Cl$ values in subducted rocks (John et al., 2010). It is also possible, however, that subduction fluids may inherit the $\delta^{37}Cl$ signature of the subducting materials because of the up to 90% Cl loss via the lizardite/chrysotile-to-antigorite transition (Kodolányi and Pettke, 2011).

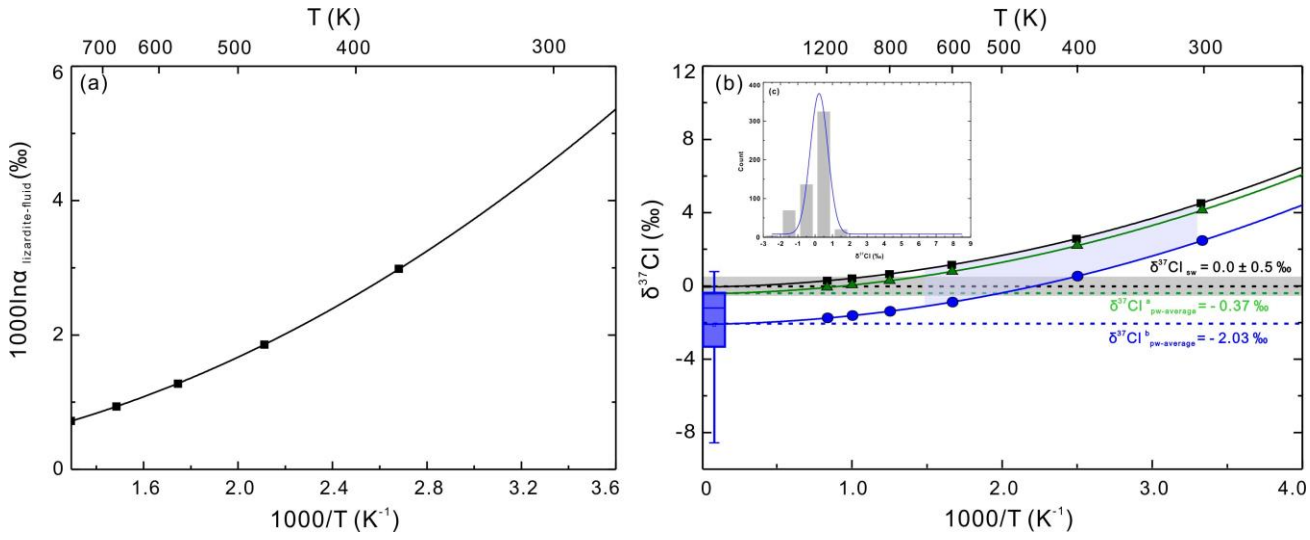

Liu, X., Wei, H.-Z., Williams-Jones, A., Ma, J., Lu, J.-J., Jiang, S.-Y., Li, Y.-C., and Dong, G., 2021,
Chlorine isotope fractionation during serpentinization and hydrothermal mineralization: A density functional theory study:
Chemical Geology, v. 581, p. 120406.

Fig. 8 (a) Temperature-dependent equilibrium chlorine isotope fractionation between lizardite and aqueous chloride; (b) Chlorine isotopic compositions for serpentine after reaction with seawater and pore water. The green shadow shows the range of $\delta^{37}Cl$ values for abyssal serpentinites. The data for $\delta^{37}Cl_{sw}$, $\delta^{37}Cl^{a}_{pw\text{-}average}$, $\delta^{37}Cl^{b}_{pw\text{-}average}$ are from Eastoe et al., 2007 and references therein; Eggenkamp, 2014 and references therein; Ransom et al., 1995; Eastoe et al., 1999, 2001; Hesse et al., 2000; Lehmann et al., 2003; Zhang et al., 2007; Goden et al., 2004; Bonifacie et al., 2007; Agrinier et al., 2019, 2021; (c) Frequency distribution of $\delta^{37}Cl$ values in serpentine from previous experimental studies (Barnes et al., 2006, 2008, 2009, 2013, Barnes and Sharp, 2006, Bonifacie et al., 2008, Wei et al., 2008, John et al., 2011, Selverstone and Sharp, 2013, Boschi et al., 2013).

4.4. Implications for chlorine cycling during subduction

Chlorine is hosted in a variety of subducting materials: sediments, pore fluids, altered oceanic crust, and serpentinite (Barnes et al., 2009). Serpentinite, as noted above, is a major H_2O reservoir in subducted slabs (e.g., Scambelluri et al., 2004; Spandler and Pirard, 2013; Yogodzinski et al., 2017), and dehydration of serpentinite causes chemical fractionation of the overlying oceanic crust in subducting slabs through fluid-rock interaction (Shimoda and Kogiso, 2019). The equilibrium chlorine isotope fractionation during serpentinization at the typical P-T conditions of the seafloor, mantle wedge and subduction zone was quantitatively estimated in this study (Fig. 9). These estimates satisfactorily reproduce the distribution of $\delta^{37}Cl$ observed in abyssal serpentinites (e.g., Barnes et al., 2006) (Fig. 8c), in the forearc mantle (Barnes and Sharp, 2006), and in eclogite-facies metasediments, which represent subducted marine sediments with the $\delta^{37}Cl$ values as high as +2.2‰ (John et al., 2010). The nominally anhydrous olivine, orthopyroxene, clinopyroxene and garnet produced by serpentinite dehydration host appreciable proportions of halogens and fluid-mobile elements that can be recycled in the deep mantle beyond arcs (Scambelluri et al., 2019). Therefore, the ability of serpentinite to record multiple interaction events with different fluids makes this rock-type essential for tracing element cycling into the mantle (Scambelluri et al., 2019 and references therein). The understanding gained of chlorine isotope fractionation during serpentinization helps

Liu, X., Wei, H.-Z., Williams-Jones, A., Ma, J., Lu, J.-J., Jiang, S.-Y., Li, Y.-C., and Dong, G., 2021,
Chlorine isotope fractionation during serpentinization and hydrothermal mineralization: A density functional theory study:
Chemical Geology, v. 581, p. 120406.

distinguish the mass transfer processes responsible for supra-subduction mantle metasomatism and arc magmatism.

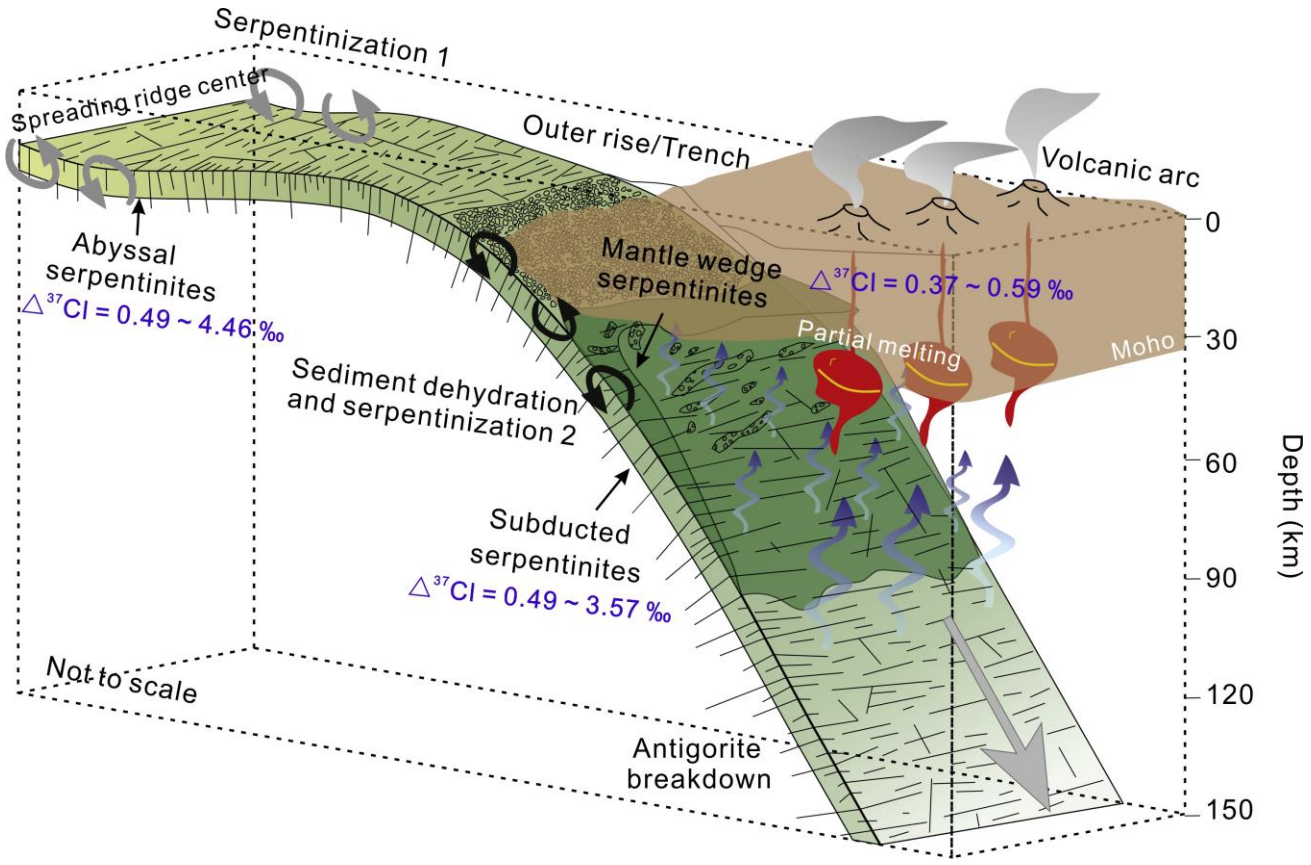

Fig. 9. A schematic diagram of the equilibrium chlorine isotope fractionation between serpentine and fluid at the seafloor, in the mantle wedge and in subduction zones (modified from Deschamps et al., 2013).

CONCLUSIONS

The temperature-dependent fractionation of chlorine isotopes during serpentinization and hydrothermal mineralization has been quantified using density functional theory calculation. In addition to hydrated chloride, the stable chlorine speciation for iron chloro-complexes in hydrothermal fluids has been simulated using *ab initio* molecular dynamics (AIMD). The evidence presented above leads to the following general conclusions:

Liu, X., Wei, H.-Z., Williams-Jones, A., Ma, J., Lu, J.-J., Jiang, S.-Y., Li, Y.-C., and Dong, G., 2021,
Chlorine isotope fractionation during serpentinization and hydrothermal mineralization: A density functional theory study:
Chemical Geology, v. 581, p. 120406.

i) The temperature-dependent chlorine isotope fractionation between lizardite and fluid can be described by the equation $1000\ln\alpha_{\text{lizardite-fluid}} = 0.4170 \times (1000/T)^2 - 0.0281\times(1000/T) + 0.0582$.

ii) The octahedral configuration is the most stable for ferrous ion chloride complexes in hydrothermal ore-forming fluid at 573.15 K and 400 MPa. The temperature dependent chlorine isotope fractionation between chlorine-bearing minerals and hydrothermal ore-forming fluids containing Fe(II) chlorocomplexes is estimated to produce $\Delta^{37}\text{Cl}_{\text{minerals-hydrothermal fluid}}$ values from -1.99 to +2.18‰. This may partly explain the large variation of δ^{37}Cl observed in magmatic-hydrothermal ore-forming fluids. The latter may also be due, however, to kinetic isotope fractionation during aqueous phase separation and crystallization. The δ^{37}Cl values of apatite-group minerals (important accessory minerals in metallic mineral deposits) may be an alternative to fluid inclusions for constraining the origin and evolution of hydrothermal fluids.

iii) Equilibrium chlorine isotope fractionation during serpentinization at the P-T conditions of the seafloor, mantle wedge and subduction zones was estimated to be 0.49 to 4.46‰, 0.37 to 0.59‰ and 0.49 to 3.57‰, respectively. The chlorine isotope composition can therefore be used to discriminate among the mass transfer processes responsible for supra-subduction mantle metasomatism and arc magmatism.

Acknowledgements:

This research was supported by the National Natural Science Foundations of China (Grants Nos. 41973002, 41830428), and the China National Space Administration (CNSA) (Grant No. D020205). We are grateful to the High Performance Computing Center (HPCC) of Nanjing University for doing the numerical calculations reported in this paper on its blade cluster system. The authors are grateful to the anonymous reviewers for their constructive and insightful comments that have improved the manuscript significantly. The careful editorial handling by the editor Prof. D. Porcelli and the guest editor Prof. Evelyn Füri is greatly appreciated.

Liu, X., Wei, H.-Z., Williams-Jones, A., Ma, J., Lu, J.-J., Jiang, S.-Y., Li, Y.-C., and Dong, G., 2021,
Chlorine isotope fractionation during serpentinization and hydrothermal mineralization: A density functional theory study:
Chemical Geology, v. 581, p. 120406.

Appendix A. Supplementary data associated with this article can be found, in the online version.

REFERENCES

Agrinier, P., Cornen, G., Beslier, M.O., 1996. Mineralogical and oxygen isotopic features of serpentinites recovered from the ocean/continent transition in the Iberia Abyssal Plain. Proc. ODP Sci. Results 149, 541-552.

Agrinier, P., Destrigneville, C., Giunta, T., Bonifacie, M., Bardoux, G., Andre, J., Lucazeau, F., 2019. Strong impact of ion filtration on the isotopic composition of chlorine in young clay-rich oceanic sediment pore fluids. Geochim. Cosmochim. Acta 245, 525-541.

Agrinier, P., Bonifacie, M., Bardoux, G., Lucazeau, F., Giunta, T., Ader, M., 2021. Chlorine isotope data of chlorides challenge the pore fluid paradigm. Geochim. Cosmochim. Acta 300, 258-278.

Alletti, M., Baker, D.R., Freda, C., 2007. Halogen diffusion in a basaltic melt. Geochim. Cosmochim. Acta 71(14), 3570-3580.

Alt, J.C., Shanks, W.C., Bach, W., Paulick, H., Garrido, C.J., Beaudoin, G., 2007. Hydrothermal alteration and microbial sulfate reduction in peridotite and gabbro exposed by detachment faulting at the Mid‐Atlantic Ridge, 15°20′N (ODP Leg 209): A sulfur and oxygen isotope study. Geochem. Geophys. Geosyst. 8(8), 1-22.

Anselmi, B., Mellini, M., Viti, C., 2000. Chlorine in the Elba, Monti Livornesi and Murlo serpentines: Evidence for sea-water interaction. Eur. J. Mineral. 12, 137-146.

Aston, F.W., 1919. The constitution of the elements. Nature 104, 393.

Balan, E., Noireaux, J., Mavromatis, V., Saldi, G.d., Montouillout, V., Blanchard, M., Pietrucci, F., Gervais, C., Rustad, J.R., Schott, J., Gaillardet, J., 2018. Theoretical isotopic fractionation between structural boron in carbonates and aqueous boric acid and borate ion. Geochim. Cosmochim. Acta 222, 117-129.

Balan, E., Créon, L., Sanloup, C., Aléon, J., Blanchard, M., Paulatto, L., Bureau, H., 2019. First-principles modeling of chlorine isotope fractionation between chloride-bearing molecules and minerals. Chem. Geol. 525, 424-434.

Balcone-Boissard, H., Baker, D.R., Villemant, B., Boudon, G., 2009. F and Cl diffusion in phonolitic melts: Influence of the Na/K ratio. Chem. Geol. 263(1-4), 89-98.

Liu, X., Wei, H.-Z., Williams-Jones, A., Ma, J., Lu, J.-J., Jiang, S.-Y., Li, Y.-C., and Dong, G., 2021,
Chlorine isotope fractionation during serpentinization and hydrothermal mineralization: A density functional theory study:
Chemical Geology, v. 581, p. 120406.

589 Banks, D.A., Green, R., Cliff, R.A., Yardley, B.W.D., 2000. Chlorine isotopes in fluid inclusions:
590 determination of the origins of salinity in magmatic fluids. Geochim. Cosmochim. Acta 64, 1785-
591 1789.
592 Barnes, J.D., Sharp, Z.D., 2006. A chlorine isotope study of DSDP/ODP serpentinized ultramafic
593 rocks: Insights into the serpentinization process. Chem. Geol. 228, 246-265.
594 Barnes, J.D., Selverstone, J., Sharp, Z.D., 2006. Chlorine isotope chemistry of serpentinites from
595 Elba, Italy, as an indicator of fluid source and subsequent tectonic history. Geochem. Geophys.
596 Geosyst. 7(8).
597 Barnes, J.D., Sharp, Z.D., Fischer, T.P., 2008. Chlorine isotope variations across the Izu-Bonin-
598 Mariana arc. Geology 36(11), 883-886.
599 Barnes, J.D., Sharp, Z.D., Fischer, T.P., Hilton, D. R., Carr, M.J., 2009. Chlorine isotope variations
600 along the Central American volcanic front and back arc. Geochem. Geophys. Geosyst. 10(11), 1-
601 17.
602 Barnes, J.D., Straub, S.M., 2010. Chlorine stable isotope variations in Izu-Bonin tephra: implications
603 for serpentinite subduction. Chem. Geol. 272, 62-74.
604 Barnes, J.D., Cisneros, M., 2012. Mineralogical control on the chlorine isotope composition of
605 altered oceanic crust. Chem. Geol. 326-327, 51-60.
606 Barnes, J.D., Eldam, R., Lee, C.-T. A., Errico, J. C., Loewy, S., Cisneros, M., 2013. Petrogenesis of
607 serpentinites from the Franciscan Complex, western California, USA. Lithos 178, 143-157.
608 Barnes, J.D., Sharp, Z.D., 2017. Chlorine isotope geochemistry. Rev. Mineral. Geochem. 82, 345-
609 378.
610 Beekman, H.E., Eggenkamp, H.G.M., Appelo, C.A.J., 2011. An integrated modelling approach to
611 reconstruct complex solute transport mechanisms-Cl and δ^{37}Cl in pore water of sediments from a
612 former brackish lagoon in The Netherlands. Appl. Geochem. 26, 257-268.
613 Berglund, M., Wieser, M.E., 2011. Isotopic compositions of the elements 2009 (IUPAC Technical
614 Report). Pure Appl. Chem. 83, 397-410.
615 Bernal, N.F., 2015. The Evolution of Magmatic-Hydrothermal Fluids as Recorded by Stable Cl
616 Isotopes and Cl/Br Elemental Ratios in Geothermal Systems, Porphyry Copper and Iron-Oxide-
617 Copper-Gold Deposits (Ph.D. Thesis). University of Alberta.
618 Bénard, B., Famin, V., Agrinier, P., Aunay, B., Lebeau, G., Sanjuan, B., Vimeux, F., Bardoux, G.,
619 Dezayes, C., 2020. Origin and fate of hydrothermal fluids at Piton des Neiges volcano (Réunion
620 Island): A geochemical and isotopic (O, H, C, Sr, Li, Cl) study of thermal springs. J. Volcanol.
621 Geoth. Res. 392, 106682.

Liu, X., Wei, H.-Z., Williams-Jones, A., Ma, J., Lu, J.-J., Jiang, S.-Y., Li, Y.-C., and Dong, G., 2021,
Chlorine isotope fractionation during serpentinization and hydrothermal mineralization: A density functional theory study:
Chemical Geology, v. 581, p. 120406.

622 Bénard, B., Famin, V., Agrinier, P., Aunay, B., Lebeau, G., Sanjuan, B., Vimeux, F., Bardoux, G.,
623 Dezayes, C., 2020. Origin and fate of hydrothermal fluids at Piton des Neiges volcano (Réunion
624 Island): A geochemical and isotopic (O, H, C, Sr, Li, Cl) study of thermal springs. J. Volcanol.
625 Geoth. Res. 392, 106682.
626 Bigeleisen, J., Mayer, M.G., 1947. Calculation of equilibrium constants for isotopic exchange
627 reactions. J. Chem. Phys. 15, 261-267.
628 Bodnar, R.J., Lecumberri-Sanchez, P., Moncada, D., Steele-MacInnis, M., 2014. Fluid inclusions in
629 hydrothermal ore deposits. In: Holland, H.D., Turekian, K.K. (Eds.), Treatise on Geochemistry
630 (2nd ed), Elsevier Ltd., Oxford, pp. 119-142.
631 Böhm, A., Schmidt, B.C., 2013. Fluorine and chlorine diffusion in phonolitic melt. Chem. Geol. 346,
632 162-171.
633 Bonifacie, M., Charlou, J.-L., Jendrzejewski, N., Agrinier, P., Donval, J.P., 2005. Chlorine isotopic
634 compositions of high temperature hydrothermal vent fluids over ridge axes. Chem. Geol. 221,
635 279–288.
636 Bonifacie, M., Jendrzejewski, N., Agrinier, P., Coleman, M., Pineau, F., Javoy, M., 2007.
637 Pyrohydrolysis-IRMS determination of silicate chlorine stable isotope compositions. Application
638 to oceanic crust and meteorite samples. Chem. Geol. 242(1-2), 187-201.
639 Bonifacie, M., Busigny, V., Mével, C., Philippot, P., Agrinier, P., Jendrzejewski, N., Scambelluri,
640 M., Javoy, M., 2008. Chlorine isotopic composition in seafloor serpentinites and high-pressure
641 metaperidotites. Insights into oceanic serpentinization and subduction processes. Geochim.
642 Cosmochim. Acta 72, 126-139.
643 Boschi, C., Bonatti, E., Ligi, M., Brunelli, D., Cipriani, A., Dallai, L., D'Orazio, M., Früh-Green,
644 G.L., Tonarini, S., Barnes, J.D., Bedini, R.M., 2013: Serpentinization of mantle peridotites along
645 an uplifted lithospheric section, Mid Atlantic Ridge at 11°N. Lithos 178, 3–23.
646 Bouvier, A.S., Manzini, M., Rose-Koga, E.F., Nichols, A.R.L., Baumgartner, L.P., 2019. Tracing of
647 Cl input into the sub-arc mantle through the combined analysis of B, O and Cl isotopes in melt
648 inclusions. Earth Planet. Sci. Lett. 507, 30-39.
649 Brugger, J., Pring, A., Reith, F., Ryan, C., Etschmann, B., Liu, W., O'Neill, B., Ngothai, Y., 2010.
650 Probing ore deposits formation: new insights and challenges from synchrotron and neutron
651 studies. Radiat. Phys. Chem. 79, 151-161.
652 Brugger, J., Liu, W., Etschmann, B., Mei, Y., Sherman, D. M., Testemale, D., 2016. A review of the
653 coordination chemistry of hydrothermal systems, or do coordination changes make ore deposits?
654 Chem. Geol. 447, 219-253.

Liu, X., Wei, H.-Z., Williams-Jones, A., Ma, J., Lu, J.-J., Jiang, S.-Y., Li, Y.-C., and Dong, G., 2021,
Chlorine isotope fractionation during serpentinization and hydrothermal mineralization: A density functional theory study:
Chemical Geology, v. 581, p. 120406.

655 Candela, P.A., Holland, H.D., 1984. The partitioning of copper and molybdenum between silicate
656 melts and aqueous fluids. Geochim. Cosmochim. Acta 48, 373–380.
657 Carlson, R.L., 2001. The abundance of ultramafic rocks in Atlantic Ocean crust. Geophys. J. Int.
658 144, 37-48
659 Carlson, R.L., Miller, D.J., 1997. A new assessment of abundance of serpentinite in the oceanic
660 crust. Geophys. Res. Lett. 24, 457-460.
661 Charlou, J.L., Fouquet, Y., Donval, J.P., Auzebde, J.M., Jean-Baptiste, P., Stievenard, M., 1996.
662 Mineral and gas chemistry of hydrothermal fluids on an ultrafast spreading ridge: East Pacific rise,
663 17° to 19° S (Naudur cruise, 1993) phase separation processes controlled by volcanic and tectonic
664 activity. J. Geophys. Res. 101, 15899-15919.
665 Charlou, J.L., Donval, J.P., Douville, E., Jean-Baptiste, P., Radford-Knoery, J., Fouquet, Y.,
666 Dapoigny, A., Stievenard, M., 2000. Compared geochemical signatures and the evolution of
667 menez gwen (37°50'N) and lucky strike (37°17'N) hydrothermal fluids, south of the azores triple
668 junction on the mid-atlantic ridge. Chem. Geol. 171(1), 49-75.
669 Chaussidon, M, Jambon A., 1984. Boron content and isotopic composition of oceanic basalts:
670 Geochemical and cosmochemical implications. Earth Planet Sci Lett 121: 277-291.
671 Chiaradia, M., Banks, D., Cliff, R., Marschik, R., de Haller, A., 2006. Origin of fluids in iron oxide–
672 copper–gold deposits: constraints from $\delta^{37}Cl$, $^{87}Sr/^{86}Sri$ and Cl/Br. Miner. Depos. 41, 565-573.
673 Chiaradia, M., Barnes, J.D., Cadet-Voisin, S., 2014. Chlorine stable isotope variations across the
674 Quaternary volcanic arc of Ecuador. Earth Planet. Sci. Lett. 396, 22-33.
675 Christensen, N.I., 1978. Ophiolites, seismic velocities and oceanic crustal structure. Tectonophysics,
676 47, 131-157.
677 Clark, S.J., Segall, M.D., Pickard C.J., Hasnip P.J., Probert, M.I.J., Refson, K., Payne, M.C., 2005.
678 First principles methods using CASTEP. Z. Krist-Cryst. Mater. 220, 567-570.
679 Czarnacki, M., Halas, S., 2012. Isotope fractionation in aqua-gas systems: Cl_2-HCl-Cl^-, Br_2-HBr-Br^-
680 and H_2S-S^{2-}. Isotopes Environ. Health Stud. 48, 55-64.
681 Debret, B.; Koga, K.T.; Nicollet, C.; Andreani, M.; Schwartz, S., 2014. F, Cl and S input via
682 serpentinite in subduction zones: Implications for the nature of the fluid released at depth. Terra
683 Nova 26, 96–101.
684 Deschamps, F., Godard, M., Guillot, S., Chauvel, C., Andreani, M., Hattori, K., Wunder, B., France,
685 L., 2012. Behavior of fluidmobile elements in serpentines from abyssal to subduction
686 environments: examples from Cuba and Dominican Republic. Chem. Geol. 312, 93–117.
687 Deschamps, F., Godard, M., Guillot, S., Hattori, K., 2013. Geochemistry of subduction zone
688 serpentinites: a review. Lithos 178(18), 96-127.

Liu, X., Wei, H.-Z., Williams-Jones, A., Ma, J., Lu, J.-J., Jiang, S.-Y., Li, Y.-C., and Dong, G., 2021,
Chlorine isotope fractionation during serpentinization and hydrothermal mineralization: A density functional theory study:
Chemical Geology, v. 581, p. 120406.

689 Dupuis, R., Benoit, M., Nardin, E., Méheut, M., 2015. Fractionation of silicon isotopes in liquids: the
690 importance of configurational disorder. Chem. Geol. 396, 239-254.
691 Eastoe, C.J., Guilbert J.M., Kaufmann R.S., 1989. Preliminary evidence for fractionation of stable
692 chlorine isotopes in ore forming hydrothermal systems. Geology 17, 285-288.
693 Eastoe, C.J., Guilbert J.M., 1992. Stable chlorine isotopes in hydrothermal processes. Geochim.
694 Cosmochim. Acta 56, 4247-4255.
695 Eastoe, C.J., Long, A., Knauth, L.P., 1999. Stable chlorine isotopes in the Palo Duro Basin, Texas:
696 evidence for preservation of Permian evaporite brines. Geochim. Cosmochim. Acta 63, 1375-
697 1382.
698 Eastoe, C.J., Peryt, T., 1999. Stable chlorine isotope evidence for non-marine chloride in Badenian
699 evaporates, Carpathian mountain region. Terra Nova 11, 118-123.
700 Eastoe, C.J., Long A., Land L.S., Kyle J.R., 2001. Stable chlorine isotopes in halite and brine from
701 the Gulf Coast Basin: brine genesis and evolution. Chem. Geol. 176, 343-360.
702 Eastoe, C.J., Peryt, T.M., Petrychenko, O.Y., Geisler-Cussey, D., 2007. Stable chlorine isotopes in
703 Phanerozoic evaporites. Appl. Geochem. 22, 575-588.
704 Eastoe, C.J., 2016. Stable chlorine isotopes in arid non-marine basins: Instances and possible
705 fractionation mechanisms. Appl. Geochem. 74, 1-12.
706 Eggenkamp, H.G.M., Kreulen, R., Koster van Groos, A.F., 1995. Chlorine stable isotope
707 fractionation in evaporites. Geochim. Cosmochim. Acta 59, 5169-5175.
708 Eggenkamp, H.G.M., Coleman M.L., 2009. The effect of aqueous diffusion on the fractionation of
709 chlorine and bromine stable isotopes. Geochim. Cosmochim. Acta 73, 3539-3548.
710 Eggenkamp, H.G.M., 2014. The geochemistry of stable chlorine and bromine isotopes. In: Hoefs,
711 J.(Ed.), Advances in Isotope Geochemistry, Springer-Verlag, Heidelberg.
712 Eggenkamp, H.G.M., Bonifacie, M., Ader, M., Agrinier, P., 2016. Experimental determination of
713 stable chlorine and bromine isotope fractionation during precipitation of salt from a saturated
714 solution. Chem. Geol. 433, 46-56.
715 Eggenkamp, H.G.M., Louvat, P., Agrinier, P., Bonifacie, M., Bekker, A., Krupenik, V., Griffioen, J.,
716 Horita, J., Brocks, J.J., Bagheri, R., 2019a. The bromine and chlorine isotope composition of
717 primary halite deposits and their significance for the secular isotope composition of seawater.
718 Geochim. Cosmochim. Acta 264, 13-29.
719 Eggenkamp, H.G.M., Louvat, P., Griffioen, J., Agrinier, P., 2019b. Chlorine and bromine isotope
720 evolution within a fully developed Upper Permian natural salt sequence. Geochim. Cosmochim.
721 Acta 245, 316-326.

Liu, X., Wei, H.-Z., Williams-Jones, A., Ma, J., Lu, J.-J., Jiang, S.-Y., Li, Y.-C., and Dong, G., 2021,
Chlorine isotope fractionation during serpentinization and hydrothermal mineralization: A density functional theory study:
Chemical Geology, v. 581, p. 120406.

722 Eggenkamp, H.G.M., Marks, M.A.W., Atanasova, P., Wenzel, T., Mark, G., 2020. Changes in
723 halogen (F, Cl, Br, and I) and S ratios in rock-forming minerals as monitors for magmatic
724 differentiation, volatile-loss, and hydrothermal overprint: The case for peralkaline systems.
725 Minerals 10, 995.
726 Evans, B.W., Hattori, K., Baronnet, A., 2013. Serpentinite: What, why, where? Elements 9, 99-106
727 Fein, J.B., Hemley, J.J., D'angelo, W.M., Komnimou, A., Sverjensky, D.A., 1992. Experimental
728 study of iron-chloride complexing in hydrothermal fluids. Geochim. Cosmochim. Acta 56, 3179-
729 3190.
730 Feisel, Y., Castro, J. M., Dingwell, D.B., 2019. Diffusion of F and Cl in dry rhyodacitic melt. Am.
731 Mineral. 104(11), 1689-1699.
732 Gammons, C.H., Williams-Jones, A.E., 1995. Hydrothermal geochemistry of electrum:
733 thermodynamic constraints. Econ. Geol. 90(2), 420-432.
734 Gammons, C.H., Yu, Y., Williams-Jones, A.E., 1997. The disproportionation of gold (I) chloride
735 complexes at 25 to 200 ℃. Geochim. Cosmochim. Acta 61(10), 1971-1983.Gleeson, S.A., Smith,
736 M.P., 2009. The sources and evolution of mineralising fluids in iron oxide-copper-gold systems,
737 Norrbotten, Sweden: Constraints from Br/Cl ratios and stable Cl isotopes of fluid inclusion
738 leachates. Geochim. Cosmochim. Acta 73, 5658-5672.
739 Hanley, J., Ames, D., Barnes, J., Sharp, Z., Guillong, M., 2011. Interaction of magmatic fluids and
740 silicate melt residues with saline groundwater in the footwall of the Sudbury Igneous Complex,
741 Ontario, Canada: New evidence from bulk rock geochemistry, fluid inclusions and stable isotopes.
742 Chem. Geol. 281, 1-25.
743 Hedenquist, J.W., Lowenstern, J.B., 1994. The role of magmas in the formation of hydrothermal ore
744 deposits. Nature 370, 519-527.
745 Heinrich, C.A., Seward, T.M., 1990. A spectrophotometric study of aqueous iron(II) chloride
746 complexing from 25 to 200 °C. Geochim. Cosmochim. Acta 54, 2207-2221.
747 Hilairet, N., Reynard, B., 2009. Stability and dynamics of serpentinite layer in subduction zone.
748 Tectonophysics 465, 24–29.
749 Hill, P.S., Schauble, E.A., Young, E.D., 2010. Effects of changing solution chemistry on Fe^{3+}/Fe^{2+}
750 isotope fractionation in aqueous Fe-Cl solutions. Geochim. Cosmochim. Acta 74, 6669-6689.
751 Huang, F., Chen, L., Wu, Z., Wang, W., 2013. First-principles calculations of equilibrium Mg
752 isotope fractionations between garnet, clinopyroxene, orthopyroxene, and olivine: Implications for
753 Mg isotope thermometry. Earth Planet. Sci. Lett. 367, 61-70.

Liu, X., Wei, H.-Z., Williams-Jones, A., Ma, J., Lu, J.-J., Jiang, S.-Y., Li, Y.-C., and Dong, G., 2021,
Chlorine isotope fractionation during serpentinization and hydrothermal mineralization: A density functional theory study:
Chemical Geology, v. 581, p. 120406.

754 Huang, F., Wu, Z., Huang, S., Wu, F., 2014. First-principles calculations of equilibrium silicon
755 isotope fractionation among mantle minerals. Geochim. Cosmochim. Acta 140, 509-520.
756 Huang, F., Zhou, C., Wang, W., Kang, J., Wu, Z., 2019. First-principles calculations of equilibrium
757 Ca isotope fractionation: Implications for oldhamite formation and evolution of lunar magma
758 ocean. Earth Planet. Sci. Lett. 510, 153-160.
759 Huang, R., Sun, W., Zhan, W., Ding, X., Zhu, J., Liu, J., 2017. Influence of temperature, pressure,
760 and fluid salinity on the distribution of chlorine into serpentine minerals. J. Asian Earth Sci. 145,
761 101-110.
762 Huang, R., Ding, X., Lin, C. T., Zhan, W., Ling, M., 2018. Effect of saline fluids on chlorine
763 incorporation in serpentine. Solid Earth Sciences, 3(3), 61-66.
764 Hyndman, R.D., Peacock, S.M., 2003. Serpentinization of the forearc mantle. Earth Planet. Sci. Lett.
765 212, 417-432.
766 John, T., Layne, G.D., Haase, K.M., Barnes, J.D., 2010. Chlorine isotope evidence for crustal
767 recycling into the Earth's mantle. Earth. Planet. Sci. Lett. 298, 175-182.
768 John, T., Scambelluri, M., Frische, M., Barnes, J.D., Bach, W., 2011. Dehydration of subducting
769 serpentinite: Implications for halogen mobility in subduction zones and the deep halogen cycle.
770 Earth. Planet. Sci. Lett. 308, 65-76.
771 Kawakatsu, H., Watada, S., 2007. Seismic evidence for deep-water transportation in the mantle.
772 Science 316, 1468–1471.
773 Kawamoto, T., Hertwig, A., Schertl, H.P., Maresch, W.V., 2018. Fluid inclusions in jadeitite and
774 jadeite-rich rock from serpentinite mélanges in northern Hispaniola: Trapped ambient fluids in a
775 cold subduction channel. Lithos 308, 227-241.
776 Kendrick, M.A., Honda, M., Pettke, T., Scambelluri, M., Phillips, D., Giuliani, A., 2013. Subduction
777 zone fluxes of halogens and noble gases in seafloor and forearc serpentinites. Earth. Planet. Sci.
778 Lett. 365, 86-96.
779 Kent, A.J.R., Peate, D.W., Newman, S., Stolper, E.M., Pearce, J.A., 2002. Chlorine in submarine
780 glasses from the Lau Basin: seawater contamination and constraints on the composition of slab-
781 derived fluids. Earth. Planet. Sci. Lett. 202, 361-377.
782 Kieffer, S.W., 1982. Thermodynamics and lattice vibrations of minerals: 5. Applications to phase
783 equilibria, isotopic fractionation, and high-pressure thermodynamic properties. Rev. Geophys. 20,
784 827-849.
785 Kodolányi, J., Pettke, T., 2011. Loss of trace elements from serpentinites during fluid-assisted
786 transformation of chrysotile to antigorite—An example from Guatemala. Chem. Geol. 284(3-4),
787 351-362.

Liu, X., Wei, H.-Z., Williams-Jones, A., Ma, J., Lu, J.-J., Jiang, S.-Y., Li, Y.-C., and Dong, G., 2021,
Chlorine isotope fractionation during serpentinization and hydrothermal mineralization: A density functional theory study:
Chemical Geology, v. 581, p. 120406.

788 Kowalski, P.M., Jahn, S., 2011. Prediction of equilibrium Li isotope fractionation between minerals
789 and aqueous solutions at high P and T: an efficient ab initio approach. Geochim. Cosmochim.
790 Acta 75, 6112-6123.
791 Kubicki, J.D., 2001. Self-consistent reaction field calculations of aqueous Al^{3+}, Fe^{3+}, and Si^{4+}:
792 calculated aqueous-phase deprotonation energies correlated with experimental ln(Ka) and pKa. J.
793 Phys. Chem. A 105, 8756-8762.
794 Lehmann, B.E., Love, A., Purtschert, R., Collon, P., Loosli, H.H., Kutschera, W., Beyerle, U.,
795 Aeschbach-Hertig, W., Kipfer, R., Frape, S.K., Herczeg, A., Moran, J., Tolstikhin, I.N., Gröning,
796 M., 2003. A comparison of groundwater dating with ^{81}Kr, ^{36}Cl and ^{4}He in four wells of the Great
797 Artesian Basin, Australia. Earth Planet Sci. Lett. 211, 237-250.
798 Li, L., Bonifacie, M., Aubaud, C., Crispi, O., Dessert, C., Agrinier, P., 2015. Chlorine isotopes of
799 thermal springs in arc volcanoes for tracing shallow magmatic activity. Earth. Planet. Sci. Lett.
800 413, 101-110.
801 Li, Y.C., Chen, H.W., Wei, H.Z., Jiang, S.Y., Palmer, M.R., T.G.M. van de Vene, Hohl, S., Lu, J.J.,
802 Ma, J., 2020. Exploration of driving mechanisms of equilibrium boron isotope fractionation in
803 tourmaline group minerals and fluid: A density functional theory study. Chem. Geol. 536,
804 119466.
805 Li, Y.C., Wei H.Z., Palmer M.R., Jiang S.Y., Liu X., Williams-Jones, A.E., Ma, J., Lu, J.J., Lin,
806 Y.B., Dong, G., 2021. Boron coordination and B/Si ordering controls over equilibrium boron
807 isotope fractionation among minerals, melts, and fluids. Chem. Geol. 561, 120030.
808 Liu, Y., Tossell, J.A., 2005. *Ab initio* molecular orbital calculations for boron isotope fractionations
809 on boric acids and borates. Geochim. Cosmochim. Acta 69, 3995-4006.
810 Liu, W.H., Etschmann, N., Foran, G., Shelley, M., Brugger, J., 2007. Deriving formation constants
811 for aqueous metal complexes from XANES spectra: Zn^{2+} and Fe^{2+} chloride complexes in
812 hypersaline solutions. Am. Mineral. 92, 761-770.
813 Liu, X., Wei, H.Z., Li, Y.C., Williams-Jones, A.E., Lu, J.J., Jiang, S.Y., Dong, G., Ma, J., Eastoe,
814 C.J., 2021. Chlorine isotope mantle heterogeneity: Constraints from theoretical first-principles
815 calculations. Chem. Geol. 572, 120193.
816 Lüdemann, H.D., Franck, E.U., 1967. Absorptionsspektren bei hohen drucken und temperaturen. I.
817 Wassrige CO_2^- und Ni_2-halogenid-losungen bis zu 500 °C und 6 kbar. Ber. Bunsen-Ges. Phys.
818 Chem. 71 (5), 455–460.
819 Lüders, V., Banks, D.A., Halbach, P., 2002. Extreme Cl/Br and $\delta^{37}Cl$ isotope fractionation in fluids
820 of modern submarine hydrothermal systems. Miner. Depos. 37, 765-771.

Liu, X., Wei, H.-Z., Williams-Jones, A., Ma, J., Lu, J.-J., Jiang, S.-Y., Li, Y.-C., and Dong, G., 2021,
Chlorine isotope fractionation during serpentinization and hydrothermal mineralization: A density functional theory study:
Chemical Geology, v. 581, p. 120406.

821 Maekawa, H., Yamamoto, K., Teruaki, I., Ueno, T., Osada, Y., 2001. Serpentinite seamounts and
822 hydrated mantle wedge in the Izu-Bonin and Mariana forearc regions. Bull. Earthq. Res. Instit.,
823 Univ. Tokyo 76, 355-366.
824 Manning, C.E., 2004. The chemistry of subduction-zone fluids. Earth. Planet. Sci. Lett. 223, 1-16.
825 Manzini, M., Bouvier, A.-S., Barnes, J. D., Bonifacie, M., Rose-Koga, E.F., Ulmer, P., Métrich, N.,
826 Bardoux, G., Williams, J., Layne, G.D., Straub, S., Baumgartner, L.P., John, T., 2017. SIMS
827 chlorine isotope analyses in melt inclusions from arc settings. Chem. Geol. 449, 112-122.
828 Marakushev, A.A., Suk, N.I., Novikov, M.P., 1997. Chloride extraction of ore-forming metals and
829 their migration from magma chambers. Dokl. Akad. Nauk 352 (1), 83-86.
830 Mei, Y., Etschmann, B., Liu, W., Sherman, D.M., Barnes, S. J., Fiorentini, M.L., Seward, T.M.,
831 Testemale, D., Brugger, J., 2015. Palladium complexation in chloride- and bisulfide-rich fluids:
832 Insights from ab initio molecular dynamics simulations and X-ray absorption spectroscopy.
833 Geochim. Cosmochim. Acta 161, 128-145.
834 Mével, C., 2003. Serpentinization of abyssal peridotites at mid-ocean ridges. C. R. Geosci. 335, 825-
835 852.
836 Miller, Y., Chaban, G.M., Zhou, J., Asmis, K.R., Neumark, D.M., Gerber, R.B., 2007. Vibrational
837 spectroscopy of $(SO_4^{2-})\cdot(H_2O)_n$ clusters, n=1-5: harmonic and anharmonic calculations and
838 experiment. J. Chem. Phys. 127, 250.
839 Nahnybida, T., Gleeson, S. A., Rusk, B. G., Wassenaar, L.I., 2009. Cl/Br ratios and stable chlorine
840 isotope analysis of magmatic–hydrothermal fluid inclusions from Butte, Montana and Bingham
841 Canyon, Utah. Miner. Depos. 44, 837-848.
842 Normand, C., Williams-Jones, A.E., 2007. Physicochemical conditions and timing of rodingite
843 formation: evidence from rodingite-hosted fluid inclusions in the JM Asbestos mine, Asbestos,
844 Québec. Geochemical Trans. 8(1), 1-19.
845 Orberger, B., Metrich, N., Mosbah, M., Catherine, M., Fouquet, Y., 1999. Nuclear microprobe
846 analysis of serpentine from the mid-atlantic ridge. Nucl. Instrum. Meth. B. 158(1-4), 575-581.
847 Pagé, L., Hattori, K., 2019. Abyssal Serpentinites: Transporting Halogens from Earth's Surface to
848 the Deep Mantle. Minerals 9(1), 61.
849 Perdew, J.P., Burke, K., Ernzerhof, M., 1996. Generalized gradient approximation made simple.
850 Phys. Rev. Lett. 77, 3685-3868.
851 Perfit, M.R., Gust, D.E., Bence, A.E., Arculus, R.J., Taylor, S.R., 1980. Chemical characteristics of
852 island arc basalts: implications for their mantle sources. Chem. Geol. 30, 227-256.

Liu, X., Wei, H.-Z., Williams-Jones, A., Ma, J., Lu, J.-J., Jiang, S.-Y., Li, Y.-C., and Dong, G., 2021,
Chlorine isotope fractionation during serpentinization and hydrothermal mineralization: A density functional theory study:
Chemical Geology, v. 581, p. 120406.

Peters, D., Bretscher, A., John, T., Scambelluri, M., Pettke, T., 2017. Fluid-mobile elements in serpentinites: Constraints on serpentinisation environments and element cycling in subduction zones. Chem. Geol. 466, 654–666.

Pinilla, C., Blanchard, M., Balan, E., Natarajan, S.K., Vuilleumier, R., Mauri, F., 2015. Equilibrium magnesium isotope fractionation between aqueous Mg^{2+} and carbonate minerals: insights from path integral molecular dynamics. Geochim. Cosmochim. Acta 163, 126-139.

Pinti, D. L., Shouakar-Stash, O., Castro, M.C., Lopez-Hernández, A., Hall, C. M., Rocher, O., Shibata, T., Ramírez-Montes, M., 2020. The bromine and chlorine isotopic composition of the mantle as revealed by deep geothermal fluids. Geochim. Cosmochim. Acta 276, 14-30.

Pye, C.C., Rudolph, W.W., 2001. An ab initio and Raman investigation of sulfate ion hydration. J. Phys. Chem. A 105, 905-912.

Ranero, C.R., Morgan, J.P., McIntosh, K., Reichert, C., 2003. Bending-related faulting and mantle serpentinization at the Middle America trench. Nature 425, 367-373.

Richard, A., Banks, D.A., Mercadier, J., Boiron, M.C., Cuney, M., Cathelineau, M., 2011. An evaporated seawater origin for the ore-forming brines in unconformity-related uranium deposits (Athabasca Basin, Canada): Cl/Br and $\delta^{37}Cl$ analysis of fluid inclusions. Geochem. Cosmochim. Acta 75, 2792–2810.

Ringwood, A.E., 1974. The petrological evolution of island arc systems. J. Geol. Soc. 130, 183–204.

Rizzo, A.L., Caracausi, A., Liotta, M., Paonita, A., Barnes, J.D., Corsaro, R.A., Martelli, M., 2013. Chlorine isotope composition of volcanic gases and rocks at mount etna (italy) and inferences on the local mantle source. Earth Planet. Sci. Lett. 371, 134-142.

Ruepke, L.H., Morgan, J.P., Hort, M., 2002. Does slab serpentinization and deserpentinization create the primary HIMU mantle component? Geochim. Cosmochim. Acta 66 (15A), 656

Rüpke, L.H., Morgan, J.P., Hort, M., Connolly, J.A.D., 2004. Serpentine and the subduction zone water cycle. Earth Planet. Sci. Lett. 223, 17–34.

Rustad, J.R., Bylaska, E.J., 2007. *Ab initio* calculation of isotopic fractionation in $B(OH)_3(aq)$ and $B(OH)_4^-(aq)$. J. Am. Chem. Soc. 129, 2222-2223.

Rustad, J.R., Nelmes, S.L., Jackson, V.E., Dixon, D.A., 2008. Quantum-chemical calculations of carbon-isotope fractionation in $CO_2(g)$, aqueous carbonate species, and carbonate minerals. J. Phys. Chem. A 112, 542-555.

Rustad, J.R., Bylaska, E.J., Jackson, V.E., Dixon, D.A., 2010. Calculation of boron-isotope fractionation between $B(OH)_3$ (aq) and $B(OH)_4^-$ (aq). Geochim. Cosmochim. Acta 74(10), 2843-2850.

Liu, X., Wei, H.-Z., Williams-Jones, A., Ma, J., Lu, J.-J., Jiang, S.-Y., Li, Y.-C., and Dong, G., 2021,
Chlorine isotope fractionation during serpentinization and hydrothermal mineralization: A density functional theory study:
Chemical Geology, v. 581, p. 120406.

886 Ryabov, V.V., Simonov, O.N., and Snisar, S.G., 2018. Fluorine and chlorine in apatites, micas, and
887 amphiboles of layered trap intrusions of the siberian platform. Russ. Geol. Geophys. 59(4), 363-
888 373.
889 Scambelluri, M., Muentener, O., Hermann, J., Piccardo, G.B., Trommsdorff, V., 1995. Subduction of
890 water into the mantle; history of an Alpine peridotite. Geology 23 (5), 459-462.
891 Scambelluri, M., Piccardo, G.B., Philippot, P., Robbiano, A., Negretti, L., 1997. High salinity fluid
892 inclusions formed from recycled seawater in deeply subducted alpine serpentinite. Earth Planet.
893 Sci. Lett. 148(3-4), 485-499.
894 Scambelluri, M., Philippot, P., 2001. Deep fluids in subduction zones. Lithos 55, 213-227.
895 Scambelluri, M., Rampone, E., Piccardo, G.B., 2001. Fluid and element cycling in subducted
896 serpentinite: a trace-element study of the Erro–Tobbio high-pressure ultramafites (Western alps,
897 NW Italy). J. Petrol. 42(1), 55-67.
898 Scambelluri, M.; Müntener, O.; Ottolini, L.; Pettke, T.T., Vannucci, R., 2004. The fate of B, Cl and
899 Li in the subducted oceanic mantle and in the antigorite breakdown fluids. Earth Planet. Sci. Lett.
900 222, 217-234
901 Scambelluri, M., Cannaò, E., Gilio, M., 2019. The water and fluid-mobile element cycles during
902 serpentinite subduction. A review. Eur. J. Mineral. 31, 405-428.
903 Schauble, E.A., Rossman, G.R., Taylor, H.P., 2003. Theoretical estimates of equilibrium chlorine-
904 isotope fractionations. Geochim. Cosmochim. Acta 67, 3267-3281.
905 Schauble, E.A., 2007. Role of nuclear volume in driving equilibrium stable isotope fractionation of
906 mercury, thallium, and other very heavy elements. Geochim. Cosmochim. Acta 71(9), 2170-2189.
907 Schauble, E.A., 2011. First-principles estimates of equilibrium magnesium isotope fractionation in
908 silicate, oxide, carbonate and hexaaquamagnesium (2+) crystals. Geochim. Cosmochim. Acta
909 75(3), 844-869.
910 Schauble, E.A., Young, E.D., 2021. Mass dependence of equilibrium oxygen isotope fractionation in
911 carbonate, nitrate, oxide, perchlorate, phosphate, silicate, and sulfate minerals. Rev. Mineral.
912 Geochem. 86(1), 137-178.
913 Scholten, L., Schmidt, C., Lecumberri-Sanchez, P., Newville, M., Lanzirotti, A., Sirbescu, M.L.C.,
914 Steele-MacInnisc, M., 2019. Solubility and speciation of iron in hydrothermal fluids. Geochim.
915 Cosmochim. Acta 252, 126-143.
916 Schwartz, S., Allemand, P., Guillot, S., 2001. Numerical model of the effect of serpentinites on the
917 exhumation of eclogitic rocks: insights from the Monviso ophiolitic massif (Western Alps).
918 Tectonophysics 42, 193–206.

Liu, X., Wei, H.-Z., Williams-Jones, A., Ma, J., Lu, J.-J., Jiang, S.-Y., Li, Y.-C., and Dong, G., 2021,
Chlorine isotope fractionation during serpentinization and hydrothermal mineralization: A density functional theory study:
Chemical Geology, v. 581, p. 120406.

Selley, D., Scott, R., Emsbo, P., Koziy, L., Hitzman, M.W., Bull, S.W., Duffett, M., Sebagenzi, S., Halpin, J., Broughton, D.W., 2018. Structural configuration of the Central African Copperbelt: roles of evaporites in structural evolution, basin hydrology, and ore location. Metals, Minerals, and Society: Society of Economic Geologists Special Publication, 115-156.

Selverstone, J., Sharp, Z.D., 2011. Chlorine isotope evidence for multicomponent mantle metasomatism in the Ivrea Zone. Earth Planet. Sci. Lett. 310, 429-440.

Selverstone, J., Sharp, Z.D., 2013. Chlorine isotope constraints on fluid-rock interactions during subduction and exhumation of the Zermatt-Saas ophiolite. Geochem. Geophys. Geosyst. 14, 4370-4391.

Seyfried, W.E.J., Foustoukos, D.I., Allen, D.E., 2004. Ultramafic-hosted hydrothermal systems at mid-ocean ridges: chemical and physical controls on pH, redox and carbon reduction reactions. In: German, C., Lin, J. (Eds.), Mid-Ocean Ridges: Hydrothermal Interactions between the Lithosphere and Oceans. American Geophysical Union Geophysical Monograph Series, pp. 267–284.

Seward, T.M., Driesner, T., 2004. Hydrothermal solution structure: experiments and computer simulations. In: Palmer, D.A., Fernandez-Prini, R., Harvey, A.H. (Eds.), Aqueous Systems at Elevated Temperatures and Pressures. Elsevier Ltd., pp. 149–182.

Seward, T.M., Williams-Jones, A.E., Migdisov, A.A., 2014. The Chemistry of Metal Transport and Deposition by Ore-Forming Hydrothermal Fluids. In: Holland, H.D., Turekian, K.K. (Eds.), Treatise on Geochemistry, second ed. Elsevier Ltd., Oxford, pp. 29–57.

Sharp, Z.D., Barnes, J.D., 2004. Water soluble chlorides in massive seafloor serpentinites: A source of chloride in subduction zones, Earth Planet. Sci. Lett. 226, 243–254.

Sharp, Z.D., Barnes, J.D., Brearley, A.J., Chaussidon, M., Fischer, T.P., Kamenetsky, V.S., 2007. Chlorine isotope homogeneity of the mantle, crust and carbonaceous chondrites. Nature 446, 1062-1065.

Sharp, Z.D., Shearer, C.K., McKeegan, K.D., Barnes, J.D., Wang, Y.Q., 2010a. The chlorine isotope composition of the moon and implications for an anhydrous mantle. Science 329(5995), 1050-1053.

Sharp, Z.D., Barnes, J.D., Fischer, T.P., Halick, M., 2010b. An experimental determination of chlorine isotope fractionation in acid systems and applications to volcanic fumaroles. Geochim. Cosmochim. Acta 74(1), 264-273.

Sharp, Z.D., Mercer, J.A., Jones, R.H., Brearley, A.J., Selverstone, J., Bekker, A., Stachel, T., 2013a. The chlorine isotope composition of chondrites and Earth. Geochim. Cosmochim. Acta 107, 189-204.

Liu, X., Wei, H.-Z., Williams-Jones, A., Ma, J., Lu, J.-J., Jiang, S.-Y., Li, Y.-C., and Dong, G., 2021,
Chlorine isotope fractionation during serpentinization and hydrothermal mineralization: A density functional theory study:
Chemical Geology, v. 581, p. 120406.

953 Sharp, Z.D., Draper, D.S., 2013b. The chlorine abundance of earth: implications for a habitable
954 planet. Earth Planet. Sci. Lett 369-370, 71-77.
955 Sharps, J.A., Brown Jr, G.E., Stebbins, J.F., 1993. Kinetics and mechanism of ligand exchange of Au
956 (III), Zn (II), and Cd (II) chlorides in aqueous solution: An NMR study from 28–98℃. Geochim.
957 Cosmochim. Acta 57(4), 721-731.
958 Shimoda, G., Kogiso, T., 2019. Effect of Serpentinite Dehydration in Subducting Slabs on Isotopic
959 Diversity in Recycled Oceanic Crust and Its Role in Isotopic Heterogeneity of the Mantle.
960 Geochem. Geophys. Geosyst. 20(11), 5449-5472.
961 Shirodkar, P.V., Banerjee, R., Xiao, Y.K., 2014. A Revisit to Vityaz Transform Fault Area, Central
962 Indian Ridge: Isotopic Evidence of Probable Hydrothermal Activity. J. Geophys. Remote Sens.
963 03.
964 Shouakar-Stash, O., Alexeev, S. V., Frape, S.K., Alexeeva, L.P., Drimmie, R.J., 2007. Geochemistry
965 and stable isotopic signatures, including chlorine and bromine isotopes, of the deep groundwaters
966 of the Siberian Platform, Russia. Appl. Geochem. 22(3), 589-605.
967 Spandler, C., Pirard, C., 2013. Element recycling from subducting slabs to arc crust: A review.
968 Lithos 170, 208–223.
969 Stolper, E., Newman, S., 1994. The role of water in the petrogenesis of Mariana through magmas.
970 Earth Planet. Sci. Lett. 121, 293-325.
971 Straub, S.M., Layne, G.D., 2003. The systematics of chlorine, fluorine, and water in Izu arc front
972 volcanic rocks: Implications for volatile recycling in subduction zones. Geochim. Cosmochim.
973 Acta67, 4179-4203.
974 Suleimenov, O.M., 2004. Simple, compact, flow-through, high temperature high pressure cell for
975 UV–vis spectrophotometry. Rev. Sci. Instrum. 75, 3363–3364.
976 Sun, W.D., Binns, R.A., Fan, A.C., Kamenetsky, V.S., Wysoczanski, R., Wei, G.J., Hu, Y.H.,
977 Arculus, R.J., 2007. Chlorine in submarine volcanic glasses from the eastern Manus basin.
978 Geochim. Cosmochim. Acta 71, 1542-1552.
979 Testemale, D., Brugger, J., Liu, W., Etschmann, B., and Hazemann, J.L., 2009. In-situ X-ray
980 absorption study of Iron(II) speciation in brines up to supercritical conditions. Chem. Geol. 264,
981 295-310.
982 Thompson, A.B., 1992. Water in the Earth's upper mantle. Nature 358 (6384), 295-302.
983 van Keken, P.E., Hacker, B.R., Syracuse, E.M., Abers, G.A., 2011. Subduction factory: 4. Depth-
984 dependent flux of H_2O from subducting slabs worldwide. J. Geophys. Res. 116.

Liu, X., Wei, H.-Z., Williams-Jones, A., Ma, J., Lu, J.-J., Jiang, S.-Y., Li, Y.-C., and Dong, G., 2021,
Chlorine isotope fractionation during serpentinization and hydrothermal mineralization: A density functional theory study:
Chemical Geology, v. 581, p. 120406.

985 Ulmer, P., Trommsdorff, V., 1995. Serpentine stability to mantle depths and subduction-related
986 magmatism. Science 268, 858-861.
987 Urey, H.C., 1947. The thermodynamic properties of isotopic substances. J. Chem. Soc. 562-581.
988 Vchirawongkwin, V., Rode, B.M., 2007. Solvation energy and vibrational spectrum of sulfate in
989 water-an ab initio quantum mechanical simulation. Chem. Phys. Lett. 443, 152–157.
990 Wallace, P.J., 2005. Volatiles in subduction zone magmas: concentrations and fluxes based on melt
991 inclusion and volcanic gas data. J. Volcanol. Geoth. Res. 140, 217–240.
992 Wei, W., Kastner, M., Spivack, A., 2008. Chlorine stable isotopes and halogen concentrations in
993 convergent margins with implications for the Cl isotopes cycle in the ocean. Earth. Planet. Sci.
994 Lett. 266, 90-104.
995 Williams-Jones, A.E., Heinrich, C.A., 2005. 100th Anniversary Special Paper: Vapor transport of
996 metals and the formation of magmatic-hydrothermal ore deposits. Econ. Geol. 100, 1287-1312.
997 Williams-Jones, A.E., Migdisov, A.A., 2014. Experimental constraints on the transport and
998 deposition of metals in ore-forming hydrothermal systems. Society of Economic Geologists, 18,
999 77-96.
1000 Wood, S.A., Samson, I.M., 1998. Solubility of ore minerals and complexation of ore metals in
1001 hydrothermal solutions. Rev. Econ. Geol. 10, 33–80.
1002 Xiao, Z., Gammons, C.H., Williams-Jones, A.E., 1998. Experimental study of copper (I) chloride
1003 complexing in hydrothermal solutions at 40 to 300℃ and saturated water vapor pressure.
1004 Geochim. Cosmochim. Acta 62(17), 2949-2964.
1005 Yardley, B.W.D., 1997. The evolution of fluids through the metamorphic cycle. In: Jamtveit, B.,
1006 Yardley, B.W.D. (Eds.), Fluid flow and transport in rocks: mechanisms and effects. Chapman and
1007 Hall, London, pp. 99-121.
1008 Yogodzinski, G.M., Kelemen, P.B., Hoernle, K., Brown, S.T., Bindeman, I., Vervoort, J.D., W.W.
1009 Sims K., Portnyagin, M., Werner, R., 2017. Sr and O isotopes in western Aleutian seafloor lavas:
1010 Implications for the source of fluids and trace element character of arc volcanic rocks. Earth
1011 Planet. Sci. Lett. 475, 169-180.
1012 Zhang, M., Frape, S. K., Love, A. J., Herczeg, A. L., Lehmann, B. E., Beyerle, U., Purtschert, R.,
1013 2007. Chlorine stable isotope studies of old groundwater, southwestern Great Artesian Basin,
1014 Australia. Appl. Geochem. 22(3), 557-574.
1015 Zhao, R.H., Pan, P.J., 2001. A spectrophotometric study of Fe(II)-chloride complexes in aqueous
1016 solutions from 10 to 100°C. Can. J. Chem. 79, 131-144.

Liu, X., Wei, H.-Z., Williams-Jones, A., Ma, J., Lu, J.-J., Jiang, S.-Y., Li, Y.-C., and Dong, G., 2021,
Chlorine isotope fractionation during serpentinization and hydrothermal mineralization: A density functional theory study:
Chemical Geology, v. 581, p. 120406.

Zhao, Y., Wei, H.Z., Liu, X., Wang, Y.J., Jiang, S.Y., Eastoe, C.J., Peryt, T.M., 2021. Isotope evidence for multiple sources of B and Cl in Middle Miocene (Badenian) evaporites, Carpathian Mountains. Appl. Geochem. 124, 104819.

Zheng, Y.F., Hermann, J., 2014. Geochemistry of continental subduction-zone fluids. Earth Planets Space 66, 9.

Zheng, Y.F., Chen, R.X., Xu, Z., Zhang, S.B., 2016. The transport of water in subduction zones. Sci. China Earth Sci. 59(4), 651-682.

Zheng, Y.F., Chen, Y.X., 2016. Continental versus oceanic subduction zones. Natl. Sci. Rev. 3(4), 495-519.

Zheng, Y.F., 2019. Subduction zone geochemistry. Geosci. Front. 10, 1223-1254.

Zheng, Y.F., Xu, Z., Chen, L., Dai, L.Q., Zhao, Z.F., 2020. Chemical geodynamics of mafic magmatism above subduction zones. J. Asian Earth Sci. 194, 104185.

Zhou, J., Santambrogio, G., Brümmer, M., Moore, D.T., Wöste, L., Meijer, G., Neumark, D.M., Asmis, K.R., 2006. Infrared spectroscopy of hydrated sulfate dianions. J. Chem. Phys. 125, 111102.

Liu, X., Wei, H.-Z., Williams-Jones, A., Ma, J., Lu, J.-J., Jiang, S.-Y., Li, Y.-C., and Dong, G., 2021,
Chlorine isotope fractionation during serpentinization and hydrothermal mineralization: A density functional theory study:
Chemical Geology, v. 581, p. 120406.